Quaternary Science Reviews 155 (2017) 50–66

Contents lists available at ScienceDirect

Quaternary Science Reviews

journal homepage: www.elsevier.com/locate/quascirev

Ice core and climate reanalysis analogs to predict Antarctic and Southern Hemisphere climate changes

P.A. Mayewski [a, b, *], A.M. Carleton [c], S.D. Birkel [a, b], D. Dixon [a], A.V. Kurbatov [a, b], E. Korotkikh [a, b], J. McConnell [d], M. Curran [e, f], J. Cole-Dai [g], S. Jiang [h], C. Plummer [e, i], T. Vance [e], K.A. Maasch [a, b], S.B. Sneed [a], M. Handley [a]

[a] Climate Change Institute, University of Maine, Orono, ME, USA
[b] School of Earth and Climate Sciences, University of Maine, Orono, ME, USA
[c] Department of Geography, The Polar Center, Pennsylvania State University, University Park, PA, USA
[d] Desert Research Institute, University of Nevada System, Reno, NV, USA
[e] Australian Antarctic Division, Kingston, Tasmania, Australia
[f] Antarctic Climate and Ecosystems Cooperative Research Centre, University of Tasmania, Hobart, Australia
[g] Department of Chemistry and Biochemistry, South Dakota State University, Brookings, SD, USA
[h] Polar Research Institute of China, Shanghai, China
[i] Institute for Marine and Antarctic Studies, University of Tasmania, Hobart, Australia

ARTICLE INFO

Article history:
Received 19 August 2016
Received in revised form
12 November 2016
Accepted 14 November 2016
Available online 23 November 2016

Keywords:
Climate change
Analogs
Ice cores
Climate reanalysis
Antarctica
Southern Hemisphere

ABSTRACT

A primary goal of the SCAR (Scientific Committee for Antarctic Research) initiated AntClim21 (Antarctic Climate in the 21st Century) Scientific Research Programme is to develop analogs for understanding past, present and future climates for the Antarctic and Southern Hemisphere. In this contribution to AntClim21 we provide a framework for achieving this goal that includes: a description of basic climate parameters; comparison of existing climate reanalyses; and ice core sodium records as proxies for the frequencies of marine air mass intrusion spanning the past ~2000 years. The resulting analog examples include: natural variability, a continuation of the current trend in Antarctic and Southern Ocean climate characterized by some regions of warming and some cooling at the surface of the Southern Ocean, Antarctic ozone healing, a generally warming climate and separate increases in the meridional and zonal winds. We emphasize changes in atmospheric circulation because the atmosphere rapidly transports heat, moisture, momentum, and pollutants, throughout the middle to high latitudes. In addition, atmospheric circulation interacts with temporal variations (synoptic to monthly scales, inter-annual, decadal, etc.) of sea ice extent and concentration. We also investigate associations between Antarctic atmospheric circulation features, notably the Amundsen Sea Low (ASL), and primary climate teleconnections including the SAM (Southern Annular Mode), ENSO (El Nĩno Southern Oscillation), the Pacific Decadal Oscillation (PDO), the AMO (Atlantic Multidecadal Oscillation), and solar irradiance variations.

1. Introduction

Recent changes in Southern Hemisphere (SH) atmospheric circulation, notably the poleward migration and intensification of the westerlies, are a consequence of both human source increases in tropospheric greenhouse gases and decreases in lower stratospheric ozone (Polvani et al., 2011). The implications for future changes in SH atmospheric circulation are highly relevant to the prediction of moisture availability and transport, storminess, marine and terrestrial ecosystem responses, sea ice extent and concentration, ocean circulation and sea level rise (Schofield et al., 2010; Spencer et al., 2014; Mayewski et al., 2015). In addition, recent research suggests East Antarctica has experienced recent rapid ice sheet changes (Greenbaum et al., 2015; Aitken et al., 2016). The Pacific coastal sector of West Antarctica and the Antarctic Peninsula, in particular, are undergoing rapid increases in glacier velocity, mass loss of ice, surface warming, and snowfall

* Corresponding author.
E-mail address: paul.mayewski@maine.edu (P.A. Mayewski).

http://dx.doi.org/10.1016/j.quascirev.2016.11.017

accumulation (ACCE, 2009; Mayewski et al., 2009; Bromwich et al., 2013; Rignot et al., 2014; Thomas et al., 2015; Pedro et al., 2016). Changes in atmospheric circulation play a key role in these cryospheric rapid increases through the poleward advection of heat and moisture (Nicolas and Bromwich, 2011), and also through the shoreward delivery of ocean heat that drives basal glacier melt (Pritchard et al., 2012). Climate modeling and analog studies of past climates agree that the recently observed poleward displacement of the westerlies will likely continue under future warming and healing of the Antarctic ozone hole (Bracegirdle et al., 2013; Mayewski et al., 2015), but they differ by suggesting either an intensification of primarily westerly winds (i.e., stronger zonal winds and reduced tropospheric wave amplitude), or intensification of primarily meridional winds (weaker westerlies and greater circulation meridionality), respectively (Bracegirdle et al., 2013; Mayewski et al., 2015, respectively).

2. Relationships between atmospheric circulation and precipitation, temperature, and sea ice concentration

Enhanced marine air mass intrusion into Antarctica is associated with increased temperature advection and moisture transport (Nicolas and Bromwich, 2011). The time-averaged (i.e., climatological) low-pressure center over the Bellingshausen-Amundsen Sea (ASL) comprises in excess of 550 singular depressions per year incoming from the Pacific (Fogt et al., 2011). This feature is associated with low temperatures from cold offshore advection and sea ice formation (Bromwich et al., 2013; Criscitiello et al., 2014; Landrum et al., 2012). Interannually, the ASL comprises a "pole of maximum variability" in the MSLP field (Connolley, 1997). When the ASL is strong (i.e., in the long-term mean and also during ENSO "cold"– La Niña– events there is enhanced cold advection and greater sea ice extent westward towards the Ross Sea sector, but warm advection and reduced ice extent occur towards the western side of the Antarctic Peninsula (e.g., Carleton et al., 1998; Turner, 2004). Conversely, when the ASL is weak, and high pressure anomalies dominate the Bellingshausen-Amundsen Sea region (often in ENSO "warm events", or El Niño), temperatures are below normal and sea ice extent is greater to the eastward in the Peninsula region (Carleton, 2003). Thus, interannual variations in Pacific sector sea ice extent and concentration accompany fluctuations in intensity of the ASL connected to the ENSO (Carleton, 1988; Carleton and Fitch, 1993; Yuan and Martinson, 2000; Holland and Kwok, 2012). Moreover, sea ice extent and concentration tend to vary inversely, especially around the time of maximum ice extent in winter and early spring. These variations are such that stronger southerly or westerly winds advect ice equatorward, reducing ice concentration due to divergence of the pack, whereas stronger and/or more persistent northerly winds (warm advection) force the sea ice edge closer to the Antarctic coast yet with greater ice concentration due to compaction of the pack accompanying ice convergence (Carleton, 1988; Yuan et al., 1999).

Climatologically, the mean sea level pressure (MSLP) field indicates a "glacial anticyclone" over the highest elevations of the Antarctic ice sheet and a low-amplitude 3-wave pattern (i.e., 3 troughs and 3 ridges) over middle and high latitudes of the Southern Hemisphere in all seasons (Fig. 1). We present MSLP rather than surface pressure (eg.,

Fogt and Stammerjohn, 2015; cf. their Figs. 6.3, 6.6) to be consistent with our correlation analyses (see below) and to better depict the teleconnection "centers of action", especially the Southern Annular Mode (SAM). Maps of geopotential height (e.g., 500 mbar) would show a broadly similar pattern to Fig. 1 for the Southern Ocean and associated sea ice areas. A poleward contraction of the circumpolar vortex in autumn and spring (MAM, SON, Fig. 1) versus an equatorward expansion in winter and summer (JJA, DJF, Fig. 1), expresses the dominant semi-annual oscillation (SAO) of the extratropical atmosphere on the SH (e.g., Van Loon, 1967; Van Loon and Rogers, 1984). In turn, the SAO interacts with the seasonal patterns of sea ice growth and decay via its influence on the surface wind stress and ocean currents (Large and van Loon, 1989; Enomoto and Ohmura, 1990). These interactions produce a highly asymmetrical temporal pattern of sea ice on the Southern Ocean; a protracted advance in the autumn and winter contrasting with a rapid decay in the spring and summer.

Because there are several climate reanalysis datasets available for investigating climatological behavior, notably atmospheric circulation, we inter-compare our results between the most commonly used climate reanalysis for the SH – ERA-Interim (ERAI) – and an ensemble average of the four leading third-generation reanalyses models (Gen 3) (Auger et al., in review). The models within Gen 3 are CFSR (Climate Forecast System Reanalysis), MERRA (Modern Era Retrospective Reanalysis for Research and Applications), JRA55 (Japanese 55-year Reanalysis), and ERAI. The MSLP behavior is captured equally well in both ERAI and Gen 3 ensemble representations (Fig. 2). Low pressure centers adjacent to East Antarctica comprise the Antarctic Circumpolar Trough (ACT) which is stable in position in DJF and JJA, but contracts slightly poleward with the SAO in the transition seasons. Therefore, the dominant MSLP system comprising the ACT is the ASL. Notably it migrates eastward from winter to summer (Fig. 1).

To investigate the potential role played by atmospheric circulation features (e.g., ASL) in precipitation, temperature and sea ice concentration anomalies around Antarctica we inter-compare these climate parameters statistically using linear correlation with the ERAI fields. We emphasize summer and winter because of the relatively strong shift in ASL longitude position between the extreme seasons.

The correlation of ERAI MSLP and precipitation (PRCP) is moderately strong (~0.5), especially in winter and in West Antarctica and near-coastal Northern Victoria Land (Fig. 3). The association is inverse over the Filchner Ronne Ice Shelf region (i.e., deeper low, more PRCP) in JJA, direct over the Bellingshausen and Amundsen Sea region (deeper low, less PRCP) in JJA, and direct over near-coastal Victoria Land (deeper low, less PRCP) in DJF. These associations also appear in the Gen 3 reanalysis ensemble (CFSR-MERRA-JRA55-ERAI) (not shown).

The correlation of ERAI MSLP and temperature at 2 m above the surface (T2) reveals moderately strong values (~0.5), mostly positive in middle to higher latitudes of the SH and negative in lower latitudes (Fig. 4). Over East Antarctica MSLP and T2 decrease together during both JJA and DJF (i.e., lower pressure with lower temperature, and vice versa). As MSLP decreases over the Filchner-Ronne region T2 rises in JJA, and albeit more weakly and over a smaller area in DJF. When MSLP decreases over the Bellingshausen-Amundsen region of West Antarctica, T2 decreases in both JJA and DJF, only over a more limited region in the summer. These extreme-season correlation patterns are similar to those generated using the Gen 3 ensemble (not shown).

The ERAI reveals areas of moderately strong (~0.5) correlation of winter sea ice concentration (SEAICE) with MSLP and both zonal and meridional winds at 10 m above the surface (U10 and V10, respectively) (Fig. 5). When MSLP is lower in the Amundsen and Ross Seas and offshore from Enderby Land in East Antarctica, SEAICE is increased. The inverse association (i.e., lower MSLP, reduced SEAICE) exists for the Antarctic Peninsula and off Queen Maud and Oates Lands in East Antarctica. With increased westerly airflow SEAICE increases in the Amundsen/Ross Seas and the Indian Ocean sector of East Antarctica, but decreases off near-coastal Northern Victoria Land and the northern tip of the Antarctic

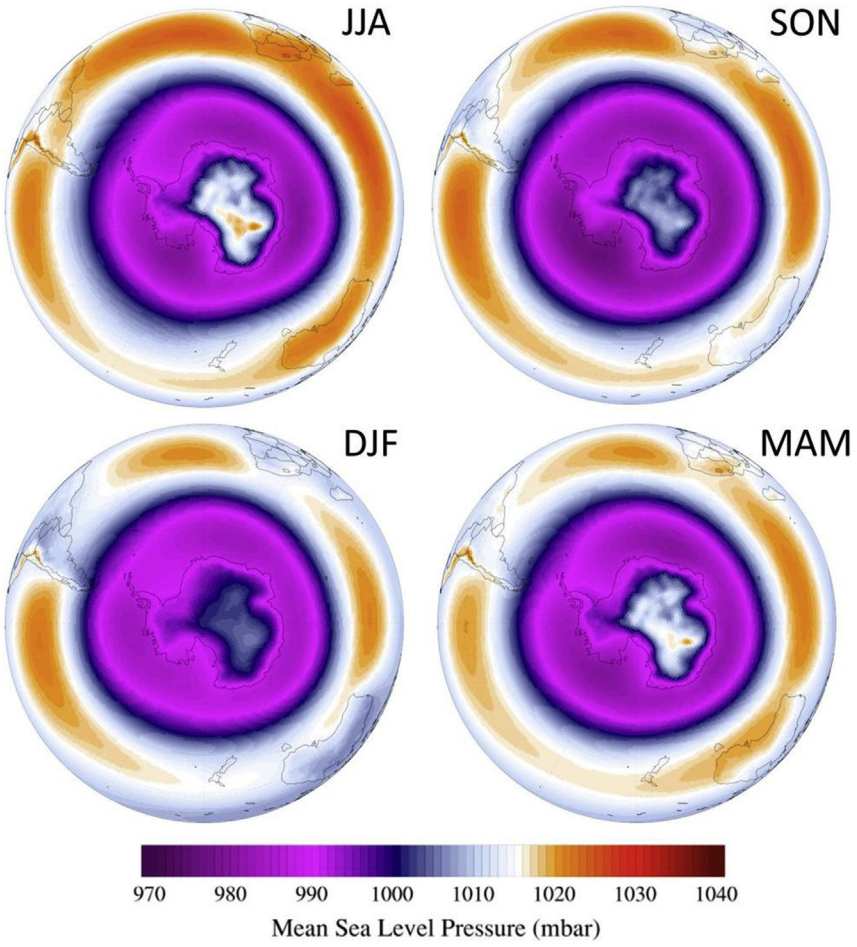

Fig. 1. MSLP during JJA, SON, DJF and MAM using ERAI (1979–2015).

Peninsula (i.e., westerly airflow associated with less SEAICE). With more equatorward-directed airflow most of the ACT experiences an increase in sea ice concentration. Closer to Antarctica (e.g., the Ross and Weddell Sea polynya regions and the Amery Ice Shelf) ice concentration decreases with offshore (i.e., equatorward) airflow. These correlation patterns are similar in the Gen 3 ensemble (not shown).

Summarizing the foregoing mapped reanalysis quantities and their correlations: (1) MSLP patterns comprise a low-amplitude 3-wave pattern in all seasons, and a poleward contraction of the circumpolar westerly vortex and ACT in the equinoctial (MAM, SON) months and the ASL changes longitudinal position between JJA and DJF; (2) PRCP is positively associated (95% confidence level) with MSLP over West Antarctica in JJA and northern/near-coastal Victoria Land in DJF; (3) T2 decreases over East Antarctica and the Amundsen-Bellingshausen region as MSLP lowers in both JJA and DJF, and in JJA T2 increases (decreases) as MSLP rises (lowers) over the Filchner-Ronne region; and (4) sea ice concentration (SEAICE) in winter increases in the vicinity of the ACT with equatorward-directed (i.e., southerly) winds, but decreases in many Antarctic embayments, and also varies with the zonal wind such that stronger westerlies accompany increased SEAICE in the ASL region and off Dronning Maud Land, but reduced SEAICE occurs off near-coastal Northern Victoria Land and the northern tip of the Peninsula.

To investigate longer-term changes in climate, notably the behavior of marine air mass intrusion over Antarctica prior to the climate reanalysis era, we investigate the climate reanalysis-calibrated ice core record of past atmospheric circulation.

3. Antarctic ice core sodium records as indicators of marine air mass advection

To infer changes in atmospheric circulation features over the past 2000 years we focus on a well-calibrated glaciochemical species, sodium, a straightforward and conservative indicator of marine source air mass intrusions: increases (decreases) indicate greater (reduced) poleward transport of warm, moist air (Legrand and Mayewski, 1997; Whitlow et al., 1992). Sodium is characterized by a winter-spring maximum accompanying more frequent and/or stronger magnitude marine air intrusions (Herron, 1982; Legrand and Delmas, 1988). In particular, ice core sodium has been interpreted as a proxy for marine source atmospheric circulation whereby increased (decreased) sodium relates to deeper (shallower) MSLP for both the ASL (West Antarctica) and the Davis Sea Low (East Antarctica) (Kreutz et al., 2000; Souney et al., 2002; Kaspari et al., 2005; Plummer et al., 2012). Recent work by Raphael et al. (2015) using the ITASE (International Trans Antarctic Scientific Expedition) West Antarctic ice core array (Dixon et al., 2012; Mayewski et al., 2013) demonstrates a 0.5 to 0.7 correlation (>95% confidence level) between mean annual ice core sodium and West Antarctic annual MSLP (1979–2001) in the Amundsen-Bellingshausen Seas and Marie Byrd Land, the ASL region. Using the ITASE West Antarctic ice core array, Sneed et al. (2011) find a

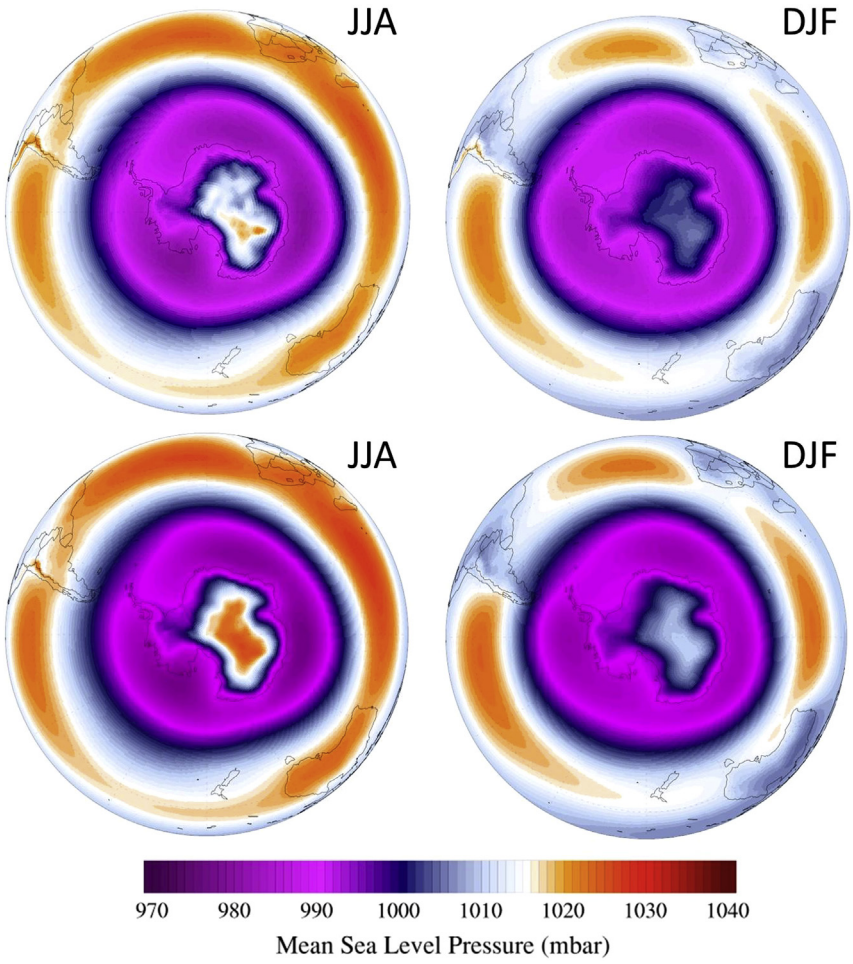

Fig. 2. MSLP during JJA and DJF using ERAI (top) and the Gen 3 Ensemble (CFSR-MERRA-JRA55-ERAI) (bottom).

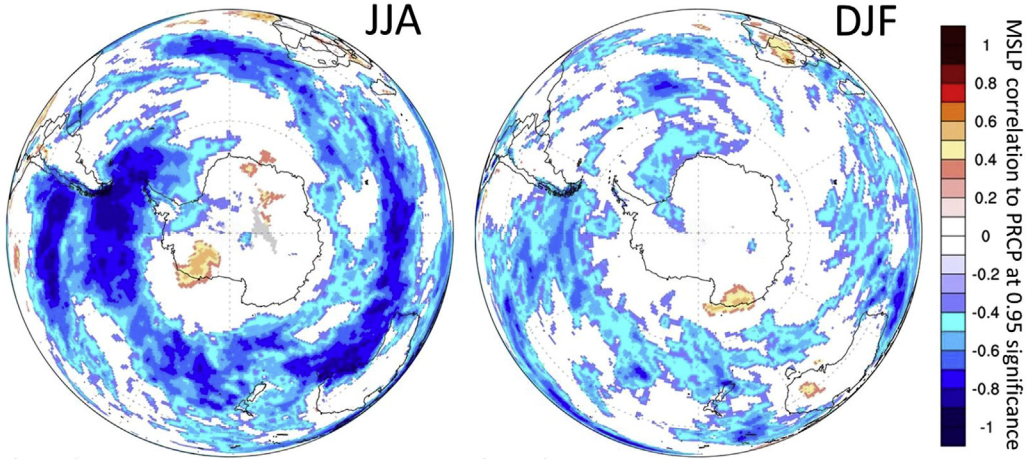

Fig. 3. Correlation between JJA and DJF MSLP compared to JJA and DJF PRCP (1979–2015) using ERAI. All filled contours are at or above 95% significance (derived using a Pearson's r significance threshold for the given sample size).

positive correlation between sodium and maximum sea ice extent in some, but not all ice cores. The positive correlation with sea ice is likely a result of strengthened atmospheric circulation at the sea ice-ocean margin. All sodium data are reported as concentration rather than sodium flux because sodium ion concentration is independent of snowfall accumulation rate (eg., Kreutz et al., 2000).

The sodium ice core records used in this study (Figs. 6 and 7) are distributed over West Antarctica as follows: RICE (Beers et al., in review), Siple Dome (SD) (Kreutz et al., 1997), WAIS Divide (WD) (Sigl et al., 2013, 2016) and East Antarctica (Law Dome (LD) (Souney et al., 2002; Plummer et al., 2012), Taylor Dome (TD) (Mayewski et al., 2012), Newall Glacier (NG) (Mayewski et al., 1995), Dominion

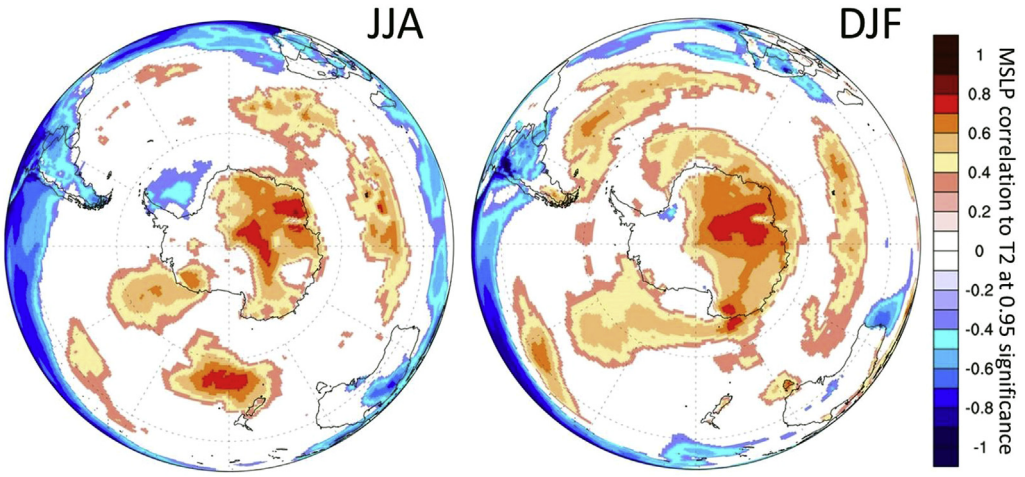

Fig. 4. Correlation between JJA and DJF MSLP compared to JJA and DJF T2 (1979–2015) using ERAI. All filled contours are at or above 95% significance (derived using a Pearson's r significance threshold for the given sample size).

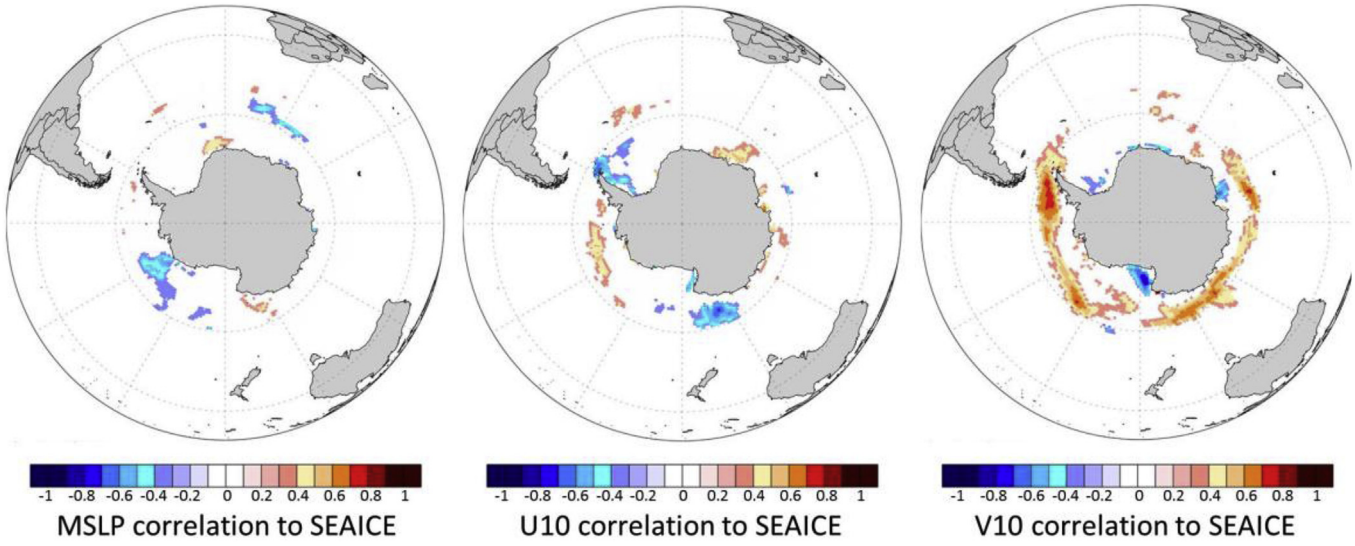

Fig. 5. Correlation between JJA values of MSLP (left), Uwind at 10 m above the surface (middle) and Vwind at 10 m above the surface (right) compared to SEAICE, respectively, using ERAI (1979–2015). All filled contours are at or above 95% significance (derived using a Pearson's r significance threshold for the given sample size).

Range (DR) (Mayewski et al., 1995, Dome A (DA) (Jiang et al., 2012)), South Pole (SP) (Korotkikh et al., in review), and Dome C (DC) (Röthlisberger et al., 2000), B40 (Sigl et al., 2013, 2014). Because we use sodium as a marine intrusion proxy we present the location of each sodium record relative to the meridional wind (v-wind) field (Fig. 6). Sodium concentrations are reported as the deviation from a 30-year mean of 10-year smoothed data allowing us to avoid differences in core-to-core sample resolution and dating, that range from 14 years per sample for Dome C to 0.3 years per sample for SP over the past 2000 years. Based on concentration and its relationship to meridional wind we bin the sodium records into three groups (Figs. 6 and 7):

(1) RICE, SD and WD are all in West Antarctica and are characterized by onshore surface airflow associated with the ASL in (Fig. 1). Sodium concentrations decrease inland and with elevation, and all sites display an increase since ~1500 years ago with RICE showing a prominent increase ~600 to ~150 years ago.

(2) B40, DA and SP are all in East Antarctica and are located in transition regions between northerly and southerly airflow. Site B40 exhibits a small increase similar in timing to RICE (both are coastal sites). DA displays a slight increase since ~1500 years ago similar to SD and WD. SP exhibits an inverse trend to both B40 and DA.

(3) DC, DR, LD, NG and TD are in East Antarctica. Sodium concentrations are generally low, with the exception of NG, a coastal site on the west coast of the Ross Ice Shelf. All sites are in regions of northerly airflow. Sites DC and TD reveal a slight increase since ~1500 years ago and a small perturbation in trend as of ~600 years ago.

In summary, several core sites reveal an increase in sodium starting ~1500 years ago with the most prominent being RICE, SD and WD in West Antarctica. Several sites reveal a more marked increase starting ~600 years ago and lasting until ~100–200 years ago, notably at RICE, SD, WD and DC, while other sites exhibit a decrease since ~600 years ago of which all are in East Antarctica

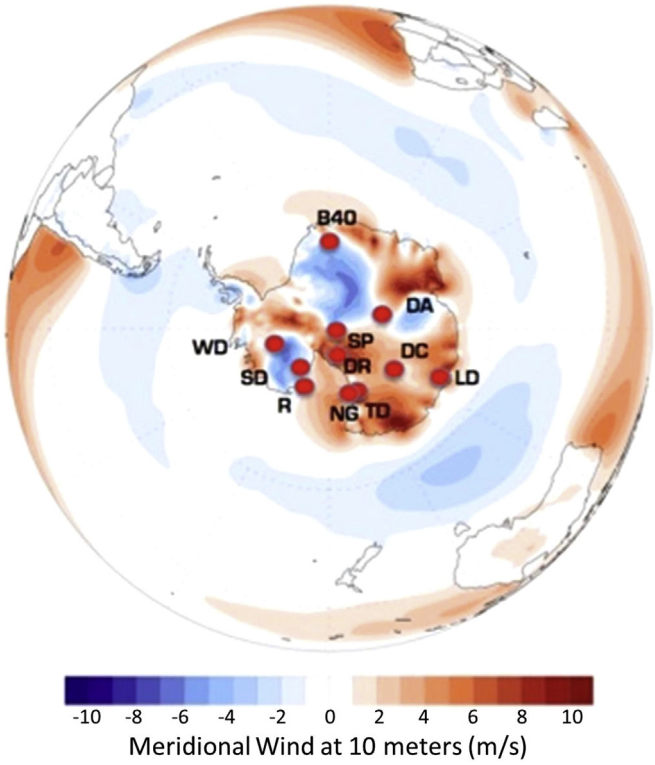

Fig. 6. Location of the sodium (ppb) records used in this study into the three groupings noted in the text: (1) WD (WAIS Divide), SD (Siple Dome) and RICE; (2) B40, DA (Dome A), and SP (South Pole); and (3) DC (Dome C), DR (Dominion Range), LD (Law Dome), NG (Newall Glacier), and TD (Taylor Dome) plotted on the ERA-Interim annual meridional wind field (1979–2015).

(B40, DA, SP and TD). Decadal scale variability over the ~2000 year record for the West Antarctic coastal sites (RICE and SD) is generally high, but for the East Antarctic sites it is relatively low with the exception of coastal site NG that does not exhibit a marked trend over the 2000 year record. We note that seasalt records from LD are used to reconstruct the Interdecadal Pacific Oscillation (IPO) - the basin-wide expression of the PDO (Vance et al., 2013, 2015).

Based on the foregoing we investigate the cause of the sodium increase at all West Antarctic and some East Antarctic sites starting ~1500 years ago; and the positive and negative departures from the ~1500 year trend as of ~600 years ago displayed by most cores.

The increase in sodium over the past ~1500 years at all West Antarctic sites is a continuation of the retreat of grounded ice and regional ice surface lowering over West Antarctica that started ~6000–7000 years ago (Conway et al., 1999), as supported by the Siple Dome sodium full Holocene record (Mayewski et al., 2012). The deglaciation was accompanied by an increased frequency of warm marine air intrusions (onshore airflow) over the Ross Sea Embayment sector of West Antarctica (Fig. 6), while East Antarctica remained isolated from these changes (Steig et al., 1998), likely due to its elevation and cold-based interior glacial anticyclone.

Departures from the ~1500-year long trend as of ~600 years ago are most prominent in the following ice cores: West Antarctica (RICE and SD) and East Antarctica (B40, DA, SP, DC, LD and TD). All cores show a sodium decrease (RICE, SD, B40, DA, SP, LD and TD) following the ~600 year ago rise, except DC and WD. The particularly prominent increase in the RICE record ~600 years ago is associated with the opening of the Ross Sea polynya that provided an additional open water source for sodium (Beers et al., in review). The DC record is relatively low-resolution and the trend is minimal. Coastal sites and those in northerly/southerly airflow transition areas exhibit decreasing sodium trends. Site WD exhibits an increase in sodium concentration as of ~1500 years ago that continues through present, suggesting either a change in the spatial extent or longitudinal location of the ASL, while the other sites reveal a weakening of the ASL since ~600 years ago. This interpretation is based on the 10-year departures from a 30-year mean; thus, the resolution does not reflect the recently observed decadal deepening of the ASL (Turner et al., 2009).

4. Past and modern atmospheric circulation analogs as a guide to near future behavior of marine air intrusions into Antarctica

4.1. Decadal and longer scale natural variability

Past climate analogs for the behavior of the ASL based on ice core data reveal increased frequencies of marine air mass intrusions in the long term, associated with West Antarctic deglaciation, and increased frequencies of marine intrusion starting ~600 years ago. These were followed by reduced marine air mass intrusion until the modern deepening of the ASL associated with the steepened polar to mid latitude thermal gradient driven by tropospheric greenhouse gas increases and stratospheric ozone loss. The ~600 year rise in sodium concentration in marine air mass "sensitive" regions (i.e., coastal and northerly/southerly airflow transition regions) is coincident with the onset of the Little Ice Age (LIA). The presence of a LIA signal in Antarctica has been previously demonstrated (eg., Kreutz et al., 1997; Bertler et al., 2011; Orsi et al., 2012), and a coincidence in timing of the onset of the LIA in Greenland and Antarctica has also been suggested (Kreutz et al., 1997; Mayewski et al., 2004). The ASL plays a key role in any discussion of not only the timing and extent of marine air mass intrusion, but also the distribution and timing of moisture and heat fluxes resulting from the ASL and other semi-permanent low pressure systems in the ACT. We caution that a strict interpretation of the LIA as meaning prevalent cold does not include the changes in the spatial extent and/or magnitude and/or temporal occurrences of the northerly winds that deliver heat and moisture to Antarctica. Therefore, the LIA should not be interpreted as purely a temperature event because LIA wind patterns are an underlying control on the spatial distribution of warming and cooling.

Examination of marine air mass intrusions based on the past ~2000 years has primary value because instrumented climate observations over Antarctica are sparse at best prior to the last few decades. However, modern analogs in the form of hemispheric-scale circulation patterns derived using climate reanalyses offer a critical guide to the future behavior of marine air intrusions, and thereby temperature changes on the continent. In the following we focus primarily on the ASL, again, because it is the dominant low pressure center in the high southern latitudes. In addition, based on previous ice core record and climate reanalysis investigations, the ASL captures a significant history of the timing and spatial extent of changes in precipitation, warm marine air intrusion and sea ice concentration and extent.

Using the ERAI climate record we next explore global and hemispheric teleconnections with the ASL, the potential forcing of this circulation feature, and derive modern analogs to help provide guidance for improving near term (next several decades) climate predictions for Antarctica and the wider Southern Hemisphere.

4.2. ASL - global climate associations

MSLP is strongly correlated to the primary pattern of atmospheric inter-annual variability in the SH, the SAM (Southern Annular Mode) (Marshall, 2003), as demonstrated using ERAI and

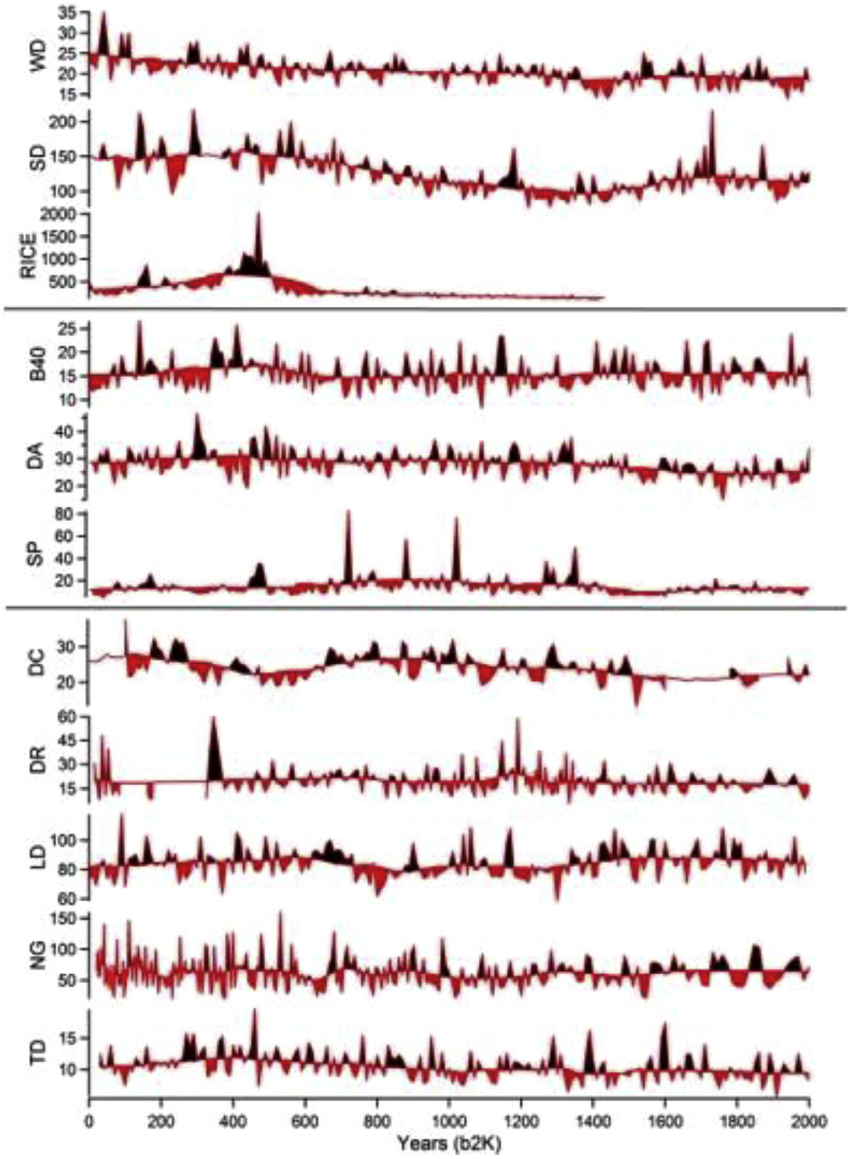

Fig. 7. Location of the sodium (ppb) records used in this study into the three groupings noted in the text: (1) WD (WAIS Divide), SD (Siple Dome) and RICE; (2) B40, DA (Dome A), and SP (South Pole); and (3) DC (Dome C), DR (Dominion Range), LD (Law Dome), NG (Newall Glacier), and TD (Taylor Dome). Positive (black) and negative (red) deviations from the 30-year mean of 10 year resampled data. (For interpretation of the references to colour in this figure legend, the reader is referred to the web version of this article.)

Gen 3 (not shown) climate reanalyses (Fig. 8). The SAM index expresses the out-of-phase relationship between MSLP anomalies over Antarctica and those over middle latitudes (e.g., Gong and Wang, 1999). Thus, when MSLP falls (rises) over Antarctica (Southern Ocean) the zonal westerlies are strong and SAM is in its positive mode; when MSLP rises (falls) over those same regions the westerlies weaken and SAM is in its negative mode. The SAM correlation pattern for JJA (Fig. 8) suggests atmospheric wavenumber one, whereby the circumpolar vortex is displaced towards the southeast South Pacific and Antarctic Peninsula (i.e., ASL region), and opposite anomalies occur in the south-east Australia/New Zealand region (e.g., Pittock, 1984; Carleton, 1989; Villalba et al., 1997). Correlation patterns in spring (SON), autumn (MAM) and summer (DJF) suggest two and three-wave patterns, respectively, but still with a primary lobe of the circumpolar vortex located over the Amundsen-Bellingshausen seas.

The ASL is strongly correlated to the tropical Pacific as seen in the association between annual Southern Hemisphere MSLP and the Southern Oscillation Index (SOI) using both ERAI (Fig. 9) and Gen 3 (not shown) and as noted in previous work (e.g., Turner et al., 2013; Schneider at al., 2012a). In particular, the pattern in the South Pacific through South Atlantic displays the Pacific-South America (PSA) wave train of opposing anomalies linking the South Pacific High, the ASL, and the Weddell Sea Low, (WSL) (e.g., Mo and Ghil, 1987; Mo and Higgins, 1998). The sub-polar features (i.e., ASL, WSL) comprise an "Antarctic Dipole" (ADP) of coupled circulation and sea-ice anomalies (Yuan and Martinson, 2000, 2001). These anomalies are such that the ASL is weaker (i.e., high pressure anomalies dominate, westerly wind speeds are reduced, less sea ice) and the WSL is stronger (low pressure anomalies, southerly winds, greater sea ice extent) during El Niño events when the eastern tropical Pacific is warmer), and vice versa in La Niña events (Carleton, 1988, 2003; Cullather et al., 1996; Turner, 2004). These positive and negative associations comprising the PSA pattern underscore the influence of modified sub-tropical and middle-latitude air masses into West Antarctica and the Antarctic

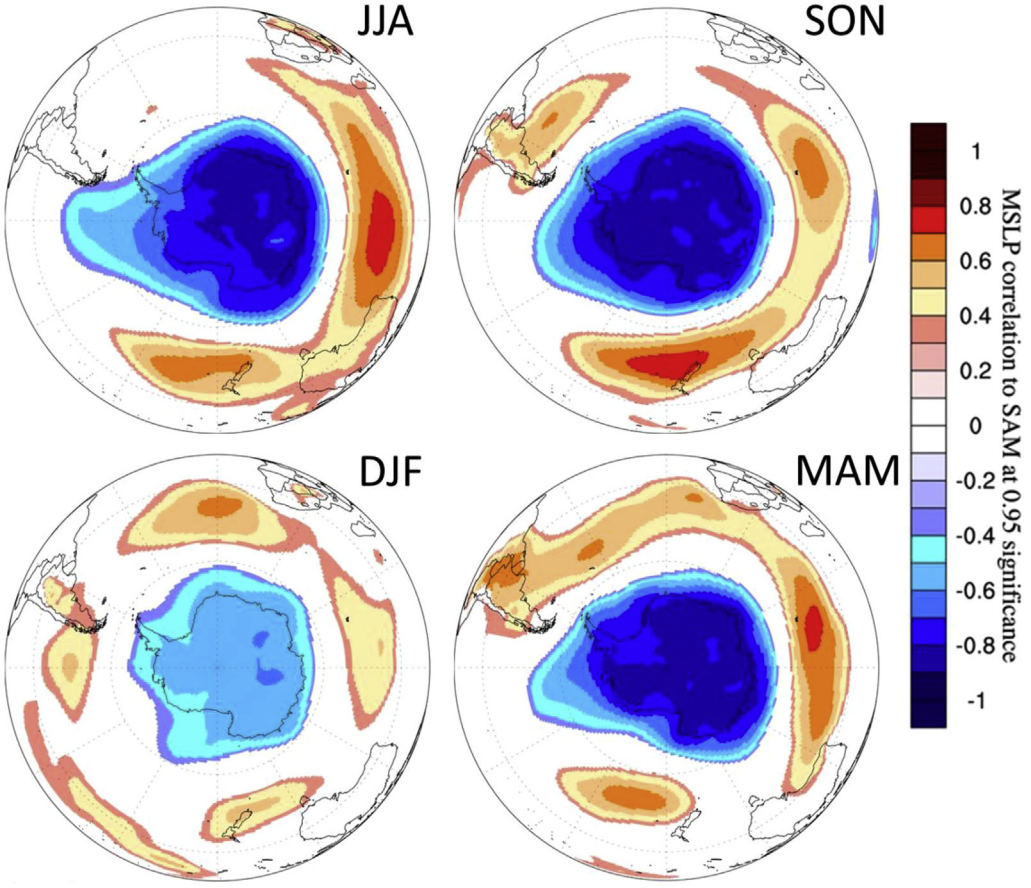

Fig. 8. Association between MSLP and SAM (from Marshall, 2003) using ERAI (1979–2012). All filled contours are at or above 95% significance (derived using a Pearson's r significance threshold for the given sample size).

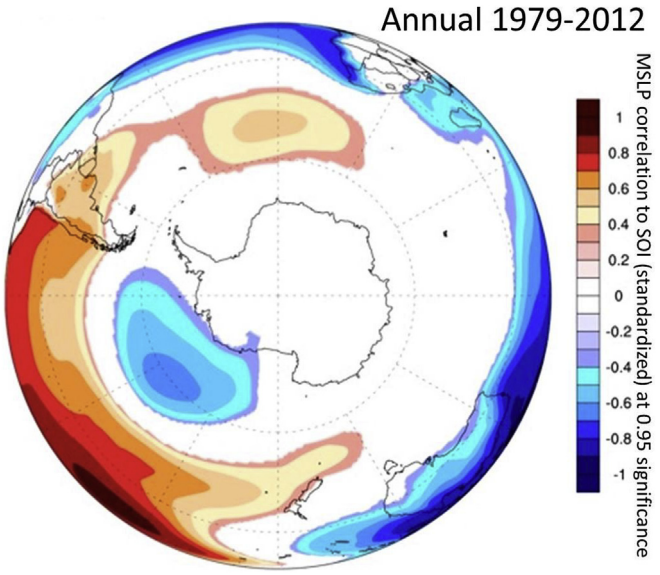

Fig. 9. Association between the ASL and ENSO using ERAI (1979–2012). All filled contours are at or above 95% significance (derived using a Pearson's r significance threshold for the given sample size).

Peninsula (Ding et al., 2011; Schneider et al., 2012b). As expected from the foregoing discussion the ASL is also correlated positively with the Pacific Decadal Oscillation (PDO), a longer period "ENSO-like" teleconnection, although the length of ERAI precludes more significant correlation with the ASL than the 0.90 confidence level attained here (Fig. 10). Although not shown we also correlated ERAI annual MSLP with annual values of the TPI IPO (a new basin-wide Tripole Index for the Interdecadal Pacific Oscillation) (Henley et al., 2015). This correlation analysis yielded a pattern similar to that of ERAI MSLP and the PDO, except that the correlation significance was weaker than 0.90 for the TPI IPO. The latter result is no doubt because TPI IPO is best used for the warm season (Vance et al., 2016) and is also not a featured teleconnection in the sequence of EOFs explaining most of the interannual variability in MSLP (Pittock, 1984; Van Loon and Rogers, 1984). The expression of Pacific Decadal variability in SH high latitudes is not restricted to the West Antarctic/ASL region, and is probably under-represented due to sparseness of both observational (prior to 1979) and ice core records in East Antarctica. Monselesan et al. (2015) showed that the mid-to high-latitudes of the SH dominate variability in sea level height and sea surface temperature anomalies in the 10–25 and 25–50 year bands, and as previously mentioned, decadal variability resembling the IPO has been detected in the LD (Indian Ocean sector) seasalt record (Vance et al., 2015).

The ASL is negatively correlated with the Atlantic Multidecadal Oscillation (AMO) (Fig. 11), an atmosphere-ocean variability mode on the order of 60–80 years most notable in the sea surface temperature (SST) field of the North Atlantic (Schlesinger and Ramankutty, 1994). Although the correlation period only covers the reanalysis era, it is interesting that moderately strong associations extend into the SH, and these also resemble the PSA pattern and ADP. This correlation may be a consequence either of AMO

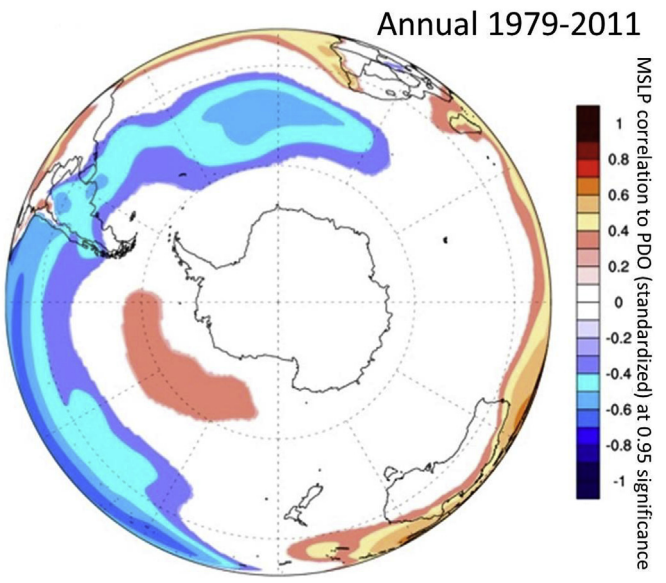

Fig. 10. Association between the ASL and PDO using ERAI MSLP and the PDO standard time series (1979–2011). All filled contours are at or above 90% significance (derived using a Pearson's r significance threshold for the given sample size).

dynamic coupling to the Atlantic Meridional Overturning Circulation (AMOC) in the global ocean (e.g., Knigh et al., 2005; Jungclaus et al., 2005) or atmospheric wind-stress patterns (Wunsch, 2006; Clement et al., 2015). We favor dominance of the wind-stress hypothesis, sustained by ocean circulation feedbacks, because the correlation operates at annual-decadal scales, too fast to be affected by ocean circulation alone, and because the wind stress association could explain the close timing of intensification of the ASL and also the Icelandic Low at the onset of the LIA, as evident in the Siple Dome and central Greenland GISP2 ice cores, respectively (Kreutz et al., 2000); and with the shift ~600 years ago in ice core sodium coastal and northerly/southerly airflow transition sites (Fig. 5, RICE, SD, B40, DA, SP, LD and TD).

Although it is clear that recent intensification of the westerlies and associated deepening of the ASL is associated with greenhouse gas warming and the Antarctic ozone hole, the ASL displays substantial variability preceding the 20th century (Mayewski et al., 2013; Dixon et al., 2012). There may also be connections with solar forcing (Mayewski et al., 2004; Maasch et al., 2005; Bertler et al., 2005) induced via associated changes in stratospheric ozone that impact latitudnal thermal gradient and therefore the strength of the polar vortex with consequences for the SAM, ASL and AMO (Fyfe et al., 1999; Shindell et al., 1999; Mayewski et al., 2006). To test for a solar-MSLP association we compare the solar cycle record with the 20th Century Climate Reanalysis MSLP fields because unlike other climate reanalyses the latter extends back to 1870. Correlation in the region of the ASL is moderate (~0.3–0.4, Fig. 12) for the full record (1871–2010) and improves around Antarctica and the Arctic for the pre-Antarctic ozone hole and pre-major greenhouse rise portion of the record (1871–1960); that is, before anthropogenic forcing impacted stratospheric ozone variability.

5. Potential scenarios for the future of the ASL with implications for Southern Hemisphere climate changes

5.1. Natural variability

Developing potential scenarios for the future of the ASL and SH climate require the highest resolution data available. Although ice core records provide the most robust reconstructions of past climate they only offer proxy reconstructions, are not equally

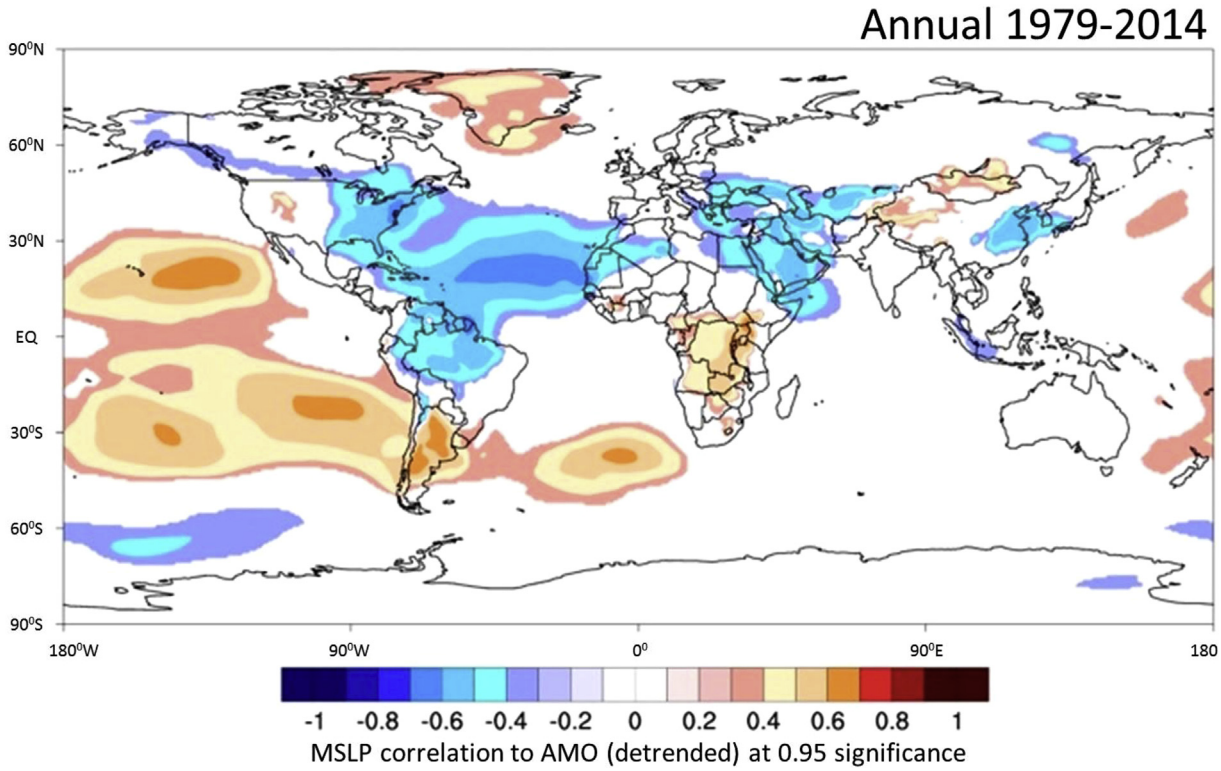

Fig. 11. Association between the AMO and the global MSLP field determined using ERAI and the standard AMO time series (1979–2014). All filled contours are at or above 95% significance (derived using a Pearson's r significance threshold for the given sample size).

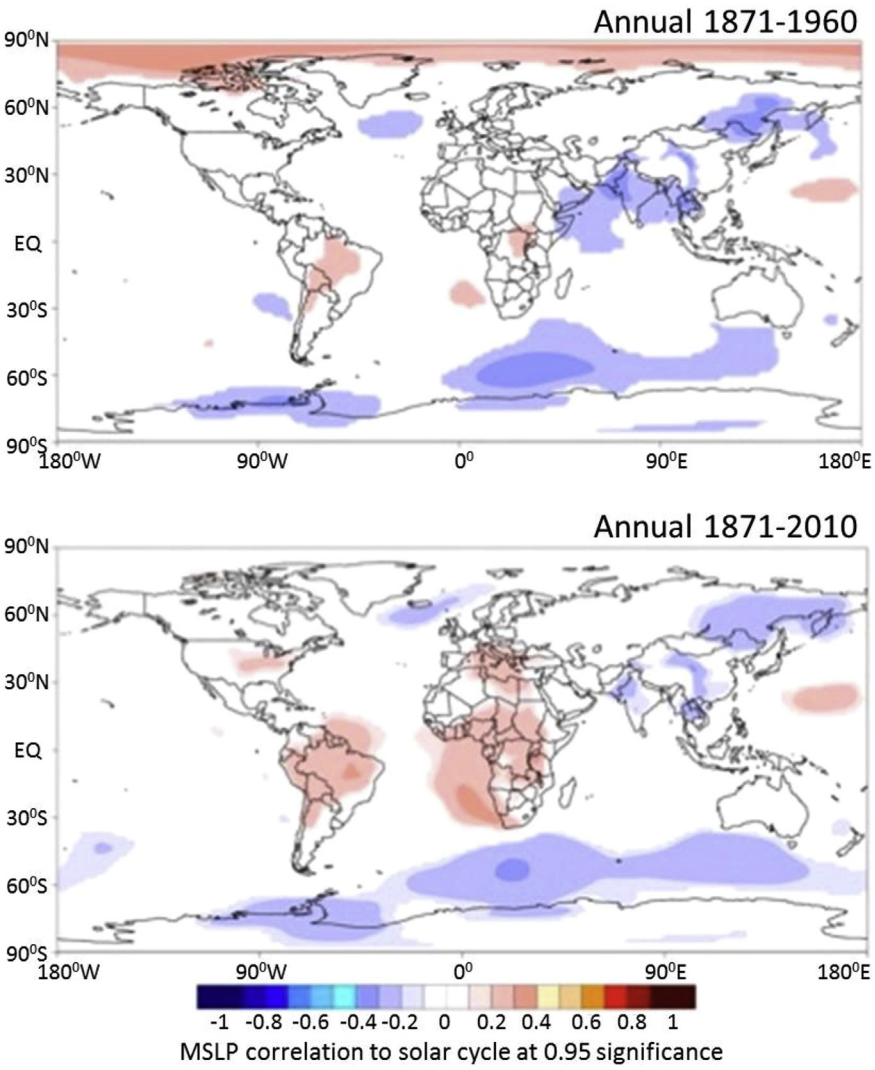

Fig. 12. Association between the solar cycle and global MSLP for the pre-Antarctic ozone hole era (1871–1960) and the full record (1871–2010) using the 20th Century Reanalysis. The International Sunspot Number is compiled by the Solar Influences Data Analysis Center in Belgium Original Source URL http://solarscience.msfc.nasa.gov/greenwch/spotnum.txt. All filled contours are at or above 95% significance (derived using a Pearson's r significance threshold for the given sample size).

spaced geographically, are relatively sparse, and are not all equally well dated, nor do they all have the same set of measurements. Notwithstanding, Antarctic ice core reconstructions offer considerable guidance in understanding past changes in, for example, temperature, winds (i.e., atmospheric circulation), precipitation, and sea ice extent. In this paper we utilized highly smoothed ice core records to avoid issues of dating quality. As noted above, examination of the last ~2000 years of ice core sodium demonstrates that West Antarctica has been in a continuing state of deglaciation since at least ~1500 years ago, and likely as of ~6000–7000 years ago based on longer ice core and glacial geologic records (Conway et al., 1999). As deglaciation continued it was accompanied by poleward contraction of the zonal westerlies and ASL, and increased frequencies of inland penetration of marine source (warm, moist) air masses, albeit with increased cooling in regions dominated by offshore airflow (e.g., westward of the ASL). West Antarctica and to a substantially lesser extent other Antarctic regions, experienced intensification in marine air mass intrusion ~600 years ago during the onset of a globally distributed LIA event, with cooling and warming dependent on the location and intensity of low pressure centers such as the ASL and Icelandic Low. This period was followed, until recent decades, by weakening of the ASL when the westerlies were more equatorward in position, and therefore lesser topographic influence of the Antarctic continent (Shulmeister et al., 2004; Stager et al., 2012).

5.2. Modern analogs for future climate

To build upon the climate reconstructions gained from the long term perspective of ice core records we use climate reanalysis data to assess the modern state of the Antarctic and Southern Ocean climate system and, most importantly, to provide guidance for assessing plausible analogs for near-term climate changes over the next 20–30 years. While the scope of this paper does not include global climate model predictions we do present a comparison for the period 1979–2005 of the ERAI and Gen 3 reanalyses with the output from two global climate models provided by the Intergovernmental Panel on Climate Change (IPCC), the Community Climate System Model (CCSM) versions CCSM3 and CCSM4). These comparisons are evaluated for monthly mean 2-meter air temperature (T2) (Fig. 13), for which there are some subtle differences. CCSM3 and CCSM4 differ over the Ross Ice Shelf with CCSM3 revealing this area to be warmer than in CCSM4. CCSM3 Ross Ice Shelf T2 is similar to the climate reanalysis reconstructions for this area, but

the warming does not extend as far poleward into West Antarctica using CCSM3 as it does using ERAI and Gen 3. Although differences between the climate reanalyses and CCSM reconstructions are relatively small they occur over a region that is potentially vulnerable to dramatic changes in the position and strength of the ASL. Therefore, we restrict our analog investigation to include only the ERAI climate reanalysis. We examine five potential analogs, all of which include known atmospheric circulation patterns: (1) the recent climate trend continues, (2) the early stages of stratospheric ozone healing, (3) a warming climate dominates, (4) meridional wind strength increases, and (5) zonal wind strength increases.

(1) **The recent climate trend continues.** This analog depicts a scenario of continued increase in greenhouse gases and a fully developed Antarctic ozone hole. Examination of the 1979–2014 ERAI T2 time series (Fig. 14) reveals a prominent change in trend around 1994 with the earlier period being generally warmer poleward of the Antarctic Circle. This trend shift coincides with a marked reversal in sign of the association between the ENSO and moisture convergence for the Pacific sector of West Antarctica (Cullather et al., 1996). Fig. 15 shows the basic climate characteristics of this analog. The westerlies strengthen as the surface pressure gradient increases between the Antarctic and middle latitudes (i.e., increasingly positive SAM; Gong and Wang, 1999) and the ASL deepens. MSLP decreases over Victoria Land weakening zonal winds, while southerly winds increase along both the west and east coasts of South America, driving cold surface ocean currents northward (Mayewski et al., 2015). T2 increases over the western Antarctic Peninsula and West Antarctic ice shelves and SST decreases across the Southern Ocean. Sea ice concentration (SEAICE) increases around all of Antarctica except the Bellingshausen Sea, northern Weddell Sea, southwest Atlantic and part of the Indian Ocean sector. PRCP decreases slightly in coastal Northern Victoria Land, southeastern-most Australia, New Zealand, and southern South America, and increases slightly in South Africa.

(2) **The initial stages of stratospheric ozone hole healing.** This analog utilizes the climate reanalysis for the early stages (1980s) of the Antarctic ozone hole. It offers a scenario for partial healing of the ozone hole. Transition time between the initial onset of Antarctic ozone depletion (1979–1985 using Total Ozone Mapping Spectrometer data) and the more pervasive ozone hole era (1985–2014) is inferred from the mean annual total ozone column time series for the hemisphere south of the Antarctic Circle using ERAI (Fig. 14). Fig. 16 captures the mean patterns of basic climate variables for this analog. Consistent with weakened MSLP gradients, zonal winds and the intensity of the ASL decrease. The exception to this pattern is the region just south of Australia,

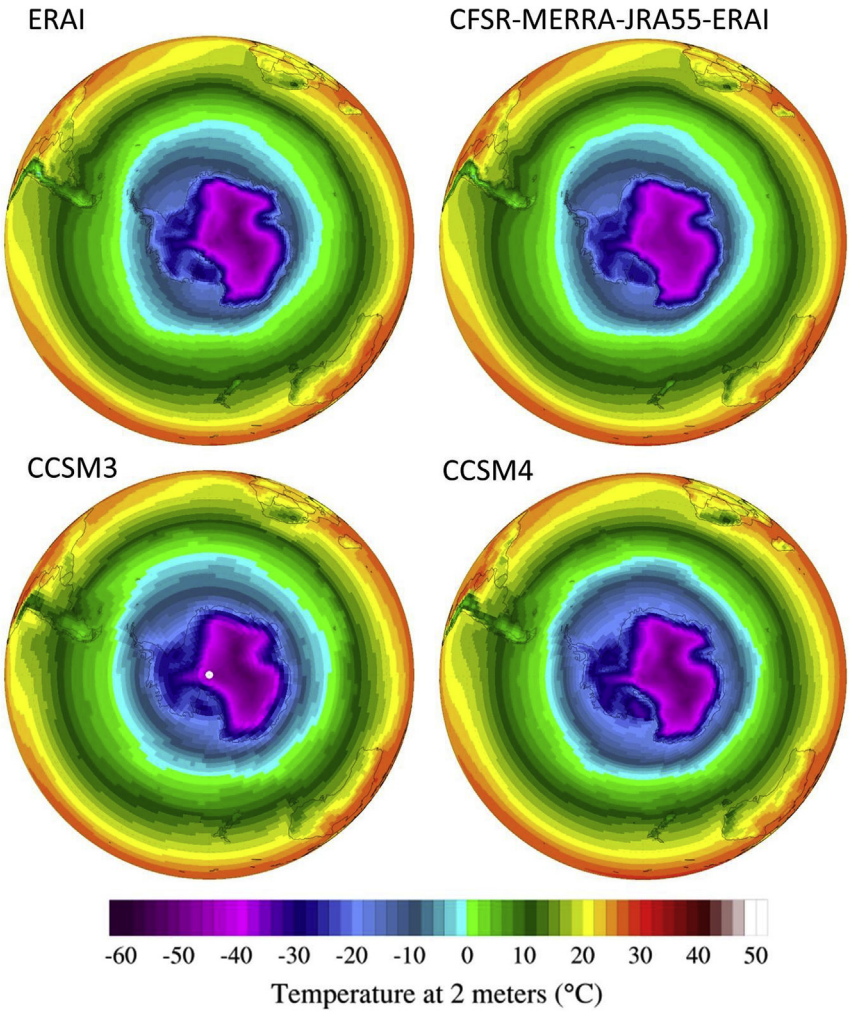

Fig. 13. Comparison of T2 between ERAI (upper left), Gen 3 Climate Reanalysis Ensemble (CFSR-MERRA-JRA55-ERAI) (upper right), CCSM3 (lower left), and CCSM4 (lower right).

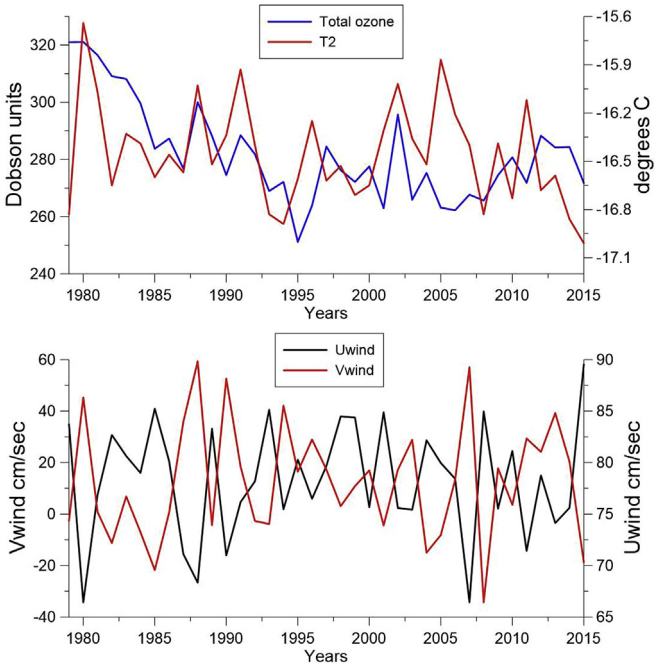

Fig. 14. Time series (1979–2015) of mean annual temperature at 2 m above the surface, mean annual total ozone column, mean annual meridional wind at 10 m above the surface, and mean annual zonal wind at 10 m above the surface using ERAI for the region south of 60 °S.

Meridional winds increase, are directed more equatorward in the northern Weddell Sea and Indian Ocean, and more poleward over the Ross Ice Shelf. T2 increases over the Ross Ice Shelf, eastern Antarctic Peninsula and much of East Antarctica with cooling over the Antarctic Peninsula and eastward. SST increases throughout much of the Southern Ocean, consistent with reduced strength of the westerlies, except for the west coast of the Antarctic Peninsula. SEAICE increases northeast of the Antarctic Peninsula, in the northern Weddell Sea, and a portion of the Indian Ocean sector of East Antarctica, but decreases around the remainder of Antarctica. PRCP decreases in southeastern Australia and South Africa and increases in southern South America and New Zealand.

(3) **A warming climate dominates.** This scenario depicts a warming climate with continued rise of greenhouse gases, and a fully developed Antarctic ozone hole. It differs from the "recent trend continues" analog by compositing separately on the warmest and the coldest years with warm (1980,1988,1991,2002, 2005, 2011) and cold (1982,1993,1994,1999, 2008, 2010) years for the region south of the Antarctic Circle chosen from the T2 time series using ERAI (Fig. 14). Fig. 17 captures the spatial patterns of climate variables. MSLP increases over the Antarctic extending into the Pacific Ocean (i.e., a weakened ASL) in warm years. This pattern is broadly similar to the El Niño composite shown by Smith and Stearns (1993). Accordingly, the westerlies south of the Antarctic Circle weaken, but they strengthen to the north, reflective of a weakened polar front jet stream (PFJ), while equatorward-directed winds increase around southern South America and off near coastal Northern Victoria Land as poleward-directed winds increase over Pacific coastal West Antarctica and eastern East Antarctica. Both T2 and SST increase across Antarctica and the Southern Ocean, except on and near the Antarctic Peninsula where T2 and SST both

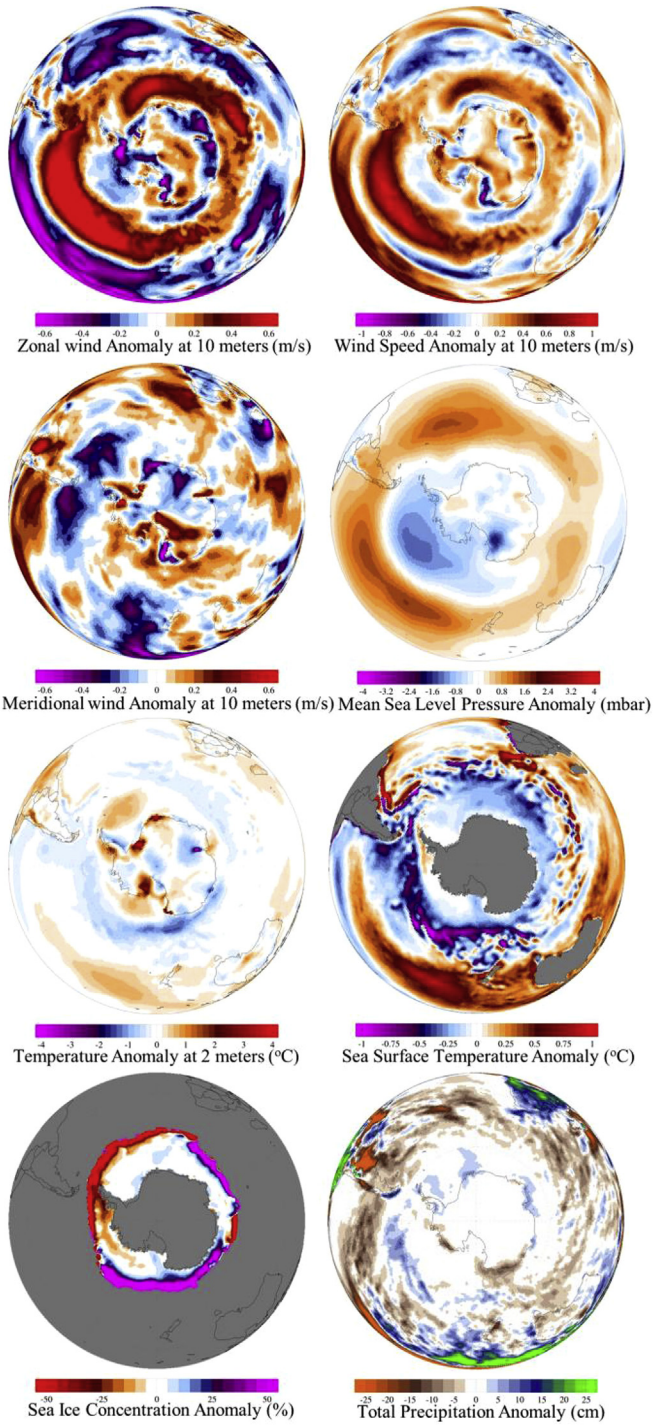

Fig. 15. Recent trend continues. Change in climate based on the period 1995–2014 minus 1979–1994 determined using ERAI anomalies for zonal wind at 10 m above the surface (m/s), wind speed at 10 m above the surface (m/s), meridional wind at 10 m above the surface (m/s), mean sea level pressure (mbar), temperature at 2 m above the surface (°C), sea surface temperature (°C), sea ice concentration (%), and total precipitation (cm).

decrease. SEAICE increases in the southwest Atlantic and western Pacific sectors and decreases off the rest of Antarctica. PRCP decreases throughout the Antarctic Peninsula and over Australia, but increases in the Ross Sea region. These composite anomaly patterns for warm minus cold years are consistent with those derived for El Niño events

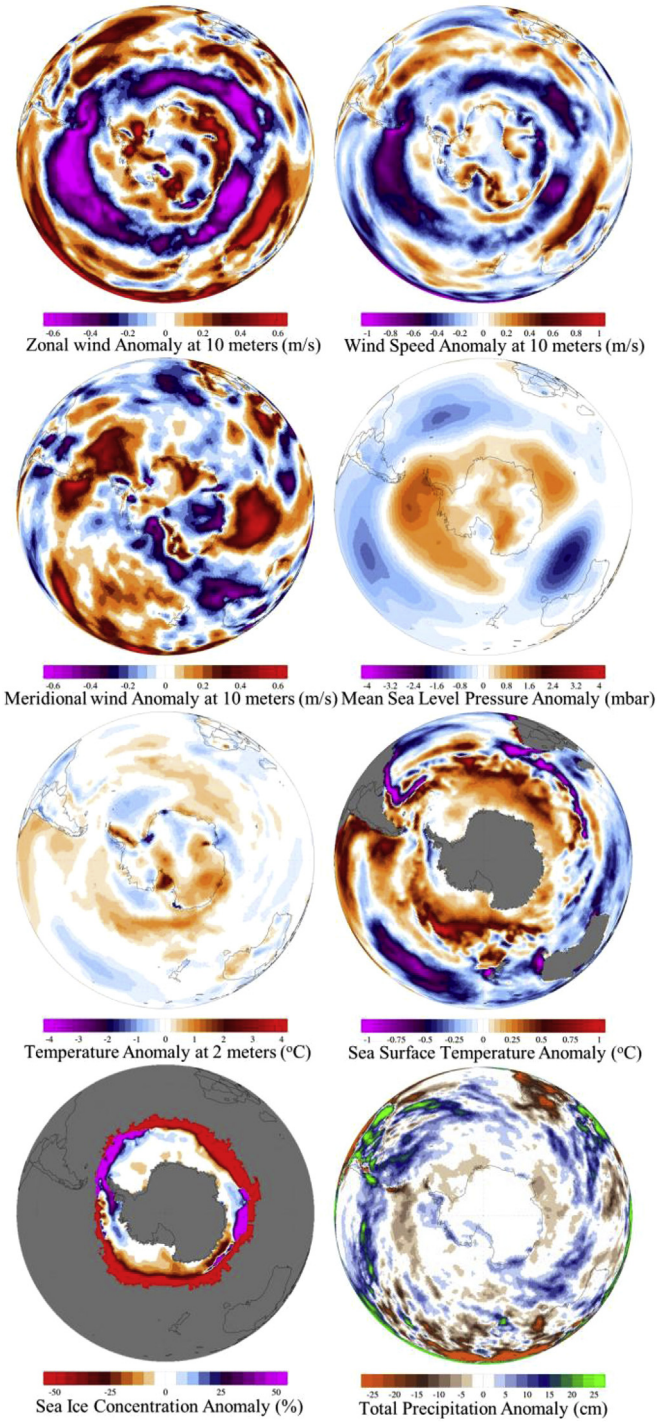

Fig. 16. Initial stages of ozone hole healing. Change in climate based on comparison of multi-year periods for the early Antarctic zone hole era (1979–1984) and full onset (1985–2014) using ERAI anomalies for zonal wind at 10 m above the surface (m/s), wind speed at 10 m above the surface (m/s), meridional wind at 10 m above the surface (m/s), mean sea level pressure (mbar), temperature at 2 m above the surface (°C), sea surface temperature (°C), sea ice concentration (%), and total precipitation (cm).

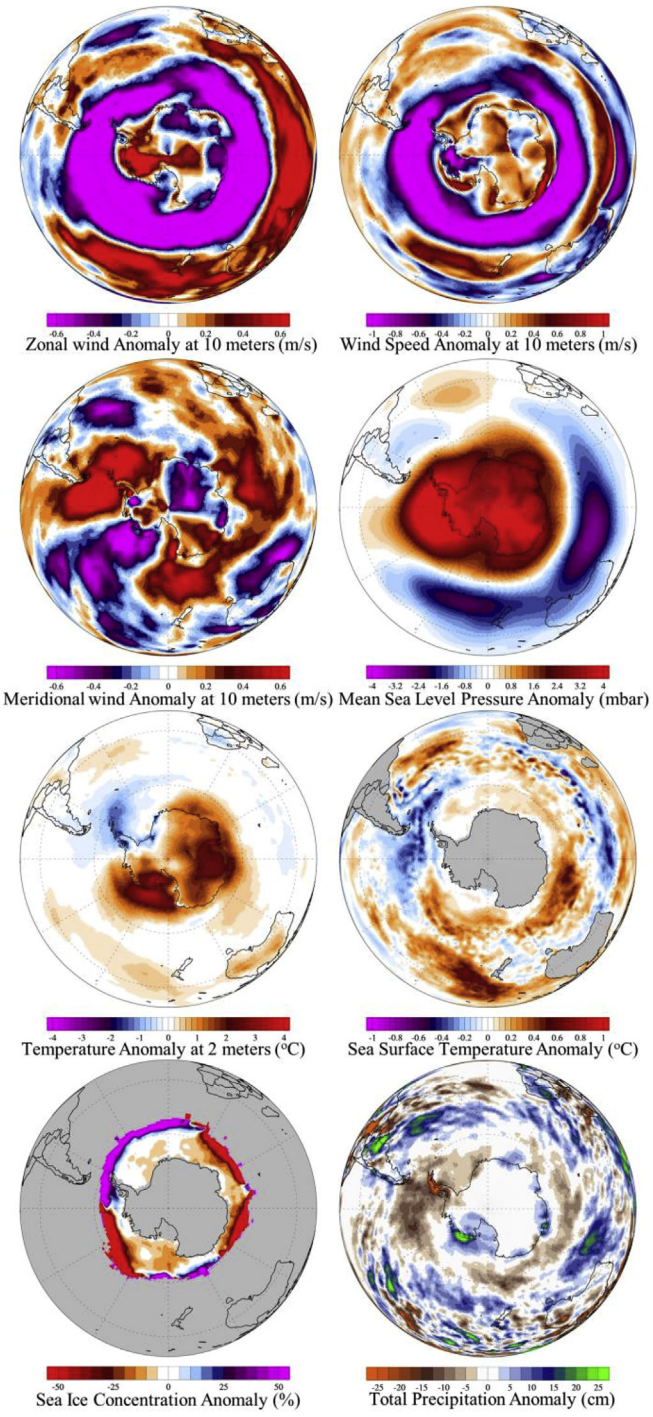

Fig. 17. Warming climate. Warmest (1980, 1988, 1991, 2002, 2005, 2011) minus coldest years (1982,1993,1994,1999, 2008, 2010) determined using ERAI anomalies for zonal wind at 10 m above the surface (m/s), wind speed at 10 m above the surface (m/s), meridional wind at 10 m above the surface (m/s), mean sea level pressure (mbar), temperature at 2 m above the surface (°C), sea surface temperature (°C), sea ice concentration (%), and total precipitation (cm).

(Carleton, 2003; Turner, 2004) superimposed on a negative SAM (Claud et al., 2009).

(4) **Meridional wind strength increases.** This analog depicts a scenario with an increase in meridional winds (both southerly and northerly) under conditions of rising greenhouse gases and an Antarctic ozone hole that is starting to heal. Years with relatively strong (1980, 1988, 1990, 1994, 2007) and relatively weak (1982, 1985, 1993, 2004, 2008) meridional winds are determined from the time series for the mean annual meridional wind field south of the Antarctic Circle from ERAI (Fig. 14). Fig. 18 shows the composite spatial differences of climate variables (strong minus weak v-winds).

MSLP rises over all of Antarctica, extending into the Bellingshausen-Amundsen Sea region (i.e., the ASL weakens), while MSLP decreases in middle latitudes, suggestive of a three-wave pattern MSLP. Accordingly, zonal winds decrease in the sub-Antarctic and increase over middle latitudes (except in the south-central South Pacific), while equatorward-directed (southerly) winds increase into South America, South Africa and the Tasman Sea, but poleward-directed (northerly) winds increase over coastal West Antarctica and from the Indian Ocean to South Pole. Patterns of T2 are consistent with meridional wind anomaly patterns; and with increases in coastal West Antarctica and the Indian Ocean sector of East Antarctic as northerly winds advect warm air inland; but decrease over the Antarctic Peninsula as southerly winds strengthen. In this scenario SST increases throughout most of the Southern Ocean except where MSLP decreases (i.e., deeper low pressure and stronger meridional winds), with especially marked upper-ocean cooling off the east coast of southern South America. Sea ice concentration (SEAICE) is in general inversely related to SST. PRCP decreases over near-coastal Northern Victoria Land and markedly over the Antarctic Peninsula and southern South America, while increasing over the Ross-Amundsen Sea coastline of West Antarctica, in southern Australia and eastward to portions of South America; resulting in a three-wave pattern combined with a negative SAM.

(5) Zonal wind strength increases.

This analog depicts a scenario of increased zonal winds under rising greenhouse gases and a fully developed Antarctic ozone hole. It essentially represents the inverse of the meridional winds scenario (i.e., stronger u = weaker v, and vice versa, averaged around the hemisphere). Years with relatively strong (1982, 1985, 1989, 1993, 1998, 2001, 2004, 2008, 2010, 2012) and relatively weak (1980, 1988, 1990, 1994, 1996, 2000, 2002, 2007, 2009, 2011) westerlies are determined from the time series for the mean annual zonal wind field south of the Antarctic Circle using ERAI (Fig. 14). Fig. 19 presents the composite spatial differences in climate variables for this analog. As expected patterns are generally the inverse of those for the meridional wind increase and warming climate analogs. Lowered MSLP over Antarctica extends into the South Pacific (i.e., a weaker continental high pressure (glacial anticyclone) and deeper ASL), while pressure in middle latitudes rises. Accordingly, the faster zonal westerlies over the sub-Antarctic, reflective of a stronger PFJ, oppose reduced westerlies in middle latitudes, and meridional winds are more northerly onto the Antarctic Peninsula (i.e., east of the deepened ASL) and near-coastal Northern Victoria Land, but southerly over West Antarctica west of the ASL and eastern East Antarctica. T2 decreases over much of Antarctica except for warming over the Antarctic Peninsula where stronger westerlies and onshore flow advects more marine air into the region. Southern Ocean SST warms, but less so than in the case of increased meridional winds, and there are regions of cooling SST. Consistent with the patterns of MSLP, meridional wind, T2 and SST, SEAICE increases in the Bellingshausen-Amundsen Sea region, in the western portion of the deepened ASL, and in the Indian Ocean sector, but decreases in other parts of Antarctica including Drake Passage. PRCP increases on the west side of the Antarctic Peninsula and decreases over the Ross Sea area. The zonal wind increase scenario resembles a composite La Niña superimposed on a positive SAM (e.g., Carleton, 2003; Claud et al., 2009).

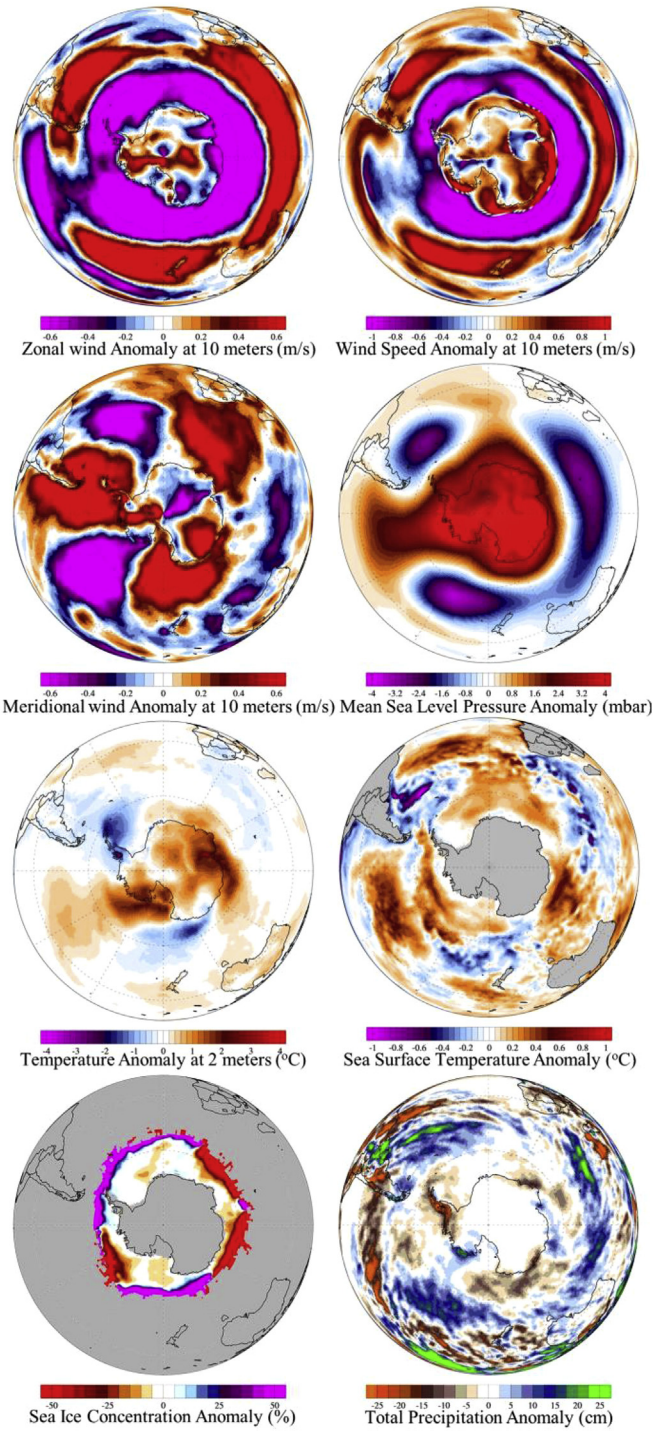

Fig. 18. Meridional wind strength increases. Strongest (1980, 1988, 1990, 1994, 2007) minus weakest (1982,1985,1993, 2004, 2008) years determined using ERAI anomalies for zonal wind at 10 m above the surface (m/s), wind speed at 10 m above the surface (m/s), meridional wind at 10 m above the surface (m/s), mean sea level pressure (mbar), temperature at 2 m above the surface (°C), sea surface temperature (°C), sea ice concentration (%), and total precipitation (cm).

6. Concluding remarks

The future of climate changes over Antarctica, the Southern Ocean, and the SH are critically intertwined. The key to predicting future climate involves assessing the behavior of major atmospheric circulation features such as the ASL that transport heat, moisture, surface ocean currents, and pollutants throughout some of the most dynamically sensitive regions of Antarctica, notably the Pacific sector of West Antarctica and the Antarctic Peninsula, and

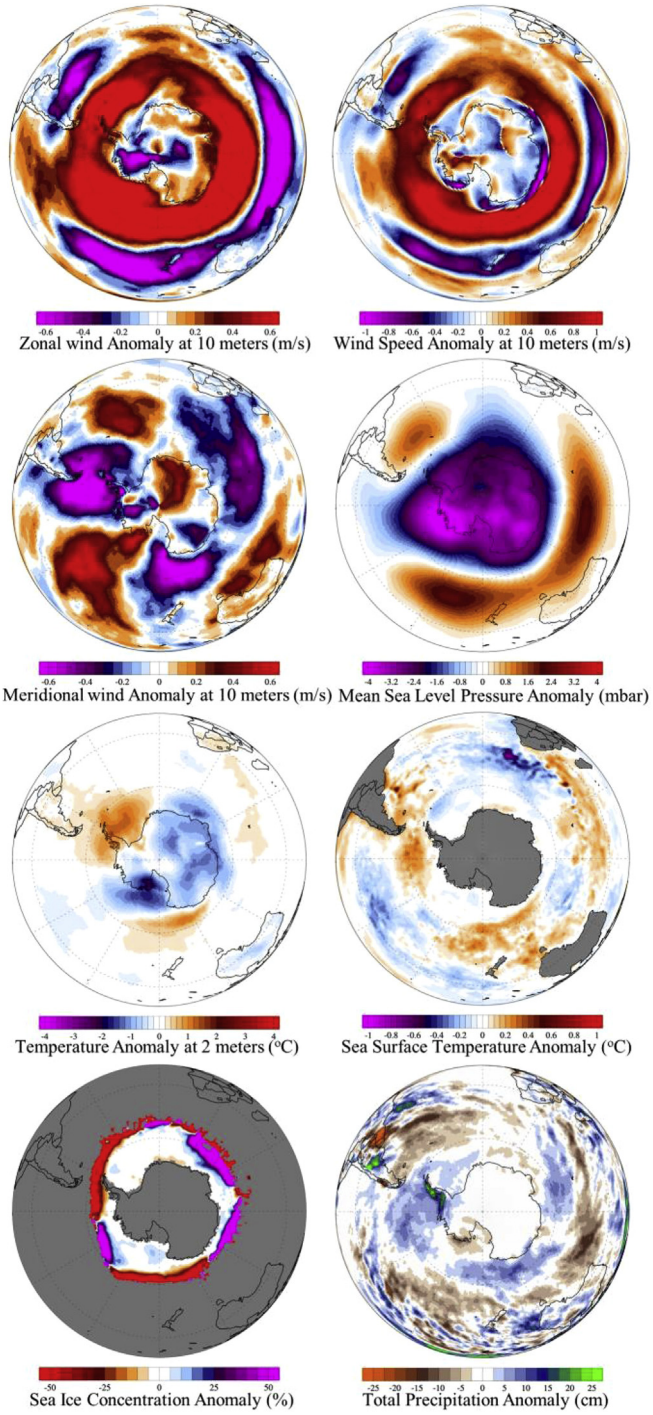

Fig. 19. Zonal wind strength increases. Strongest (1982, 1985, 1989, 1993, 1998, 2001, 2004, 2008, 2010, 2012) minus weakest (1980, 1998, 1990, 1994, 1996, 2000, 2002, 2007, 2009, 2011) years determined using ERAI anomalies for zonal wind at 10 m above the surface (m/s), wind speed at 10 m above the surface (m/s), meridional wind at 10 m above the surface (m/s), mean sea level pressure (mbar), temperature at 2 m above the surface (°C), sea surface temperature (°C), sea ice concentration (%), and total precipitation (cm).

near-coastal Northern Victoria Land. Analogs based on natural versus modern human forced climate era records provide near-term (next 20–30 years) plausible examples for future climate.

The natural variability analog presented is based on decadal and longer interpretations of eleven ~2000 year long ice core sodium proxies for marine air intrusion into Antarctica. These records emphasize the dynamic response of West Antarctica to long-term climate forcing while much of East Antarctica, exclusive of near-coastal Northern Victoria Land, has remained relatively stable with respect to the frequency of marine air mass intrusion. Most of the eleven ice core marine proxy records reveal a change close to the LIA onset (~600 years ago). Although some of the ~2000 year long ice core records overlap the 1979–2014 climate reanalysis era they do not provide as robust a scheme for investigating analogs during the era of natural and anthropogenic forcing interplay, so only climate reanalyses are utilized for this most recent period. The limitation with these analog examples is that they do not cover the pre-Antarctic ozone hole era; only the early onset era. As a consequence the ozone healing and warming climate analogs likely underestimate what will be the real climate responses, but they do provide plausible analogs for near-term future climate changes. This assertion is bolstered by the analogs' resemblance to significant SH teleconnection patterns, particularly ENSO (El Niño, La Niña) and SAM, and the internal consistency of the anomalies (e.g., T2, v-winds, SEAICE) or composite differences of the climate variables (e.g., Carleton, 1989). While there are certainly more complications involved in understanding future climate the analog scenarios we present have potential for application to a variety of climate related investigations including: ice sheet dynamics, water resource availability, storm potential, climate instability, potential for abrupt climate change, sea ice conditions (concentration, areal extent, thickness), and both terrestrial and marine ecosystem responses. For more in depth viewing these analogs can be examined at seasonal and monthly scales by using the Climate Change Institute's Climate Reanlyzer™ software (http://climatechange.umaine.edu/).

Acknowledgments

Ice core sodium records used in this study were recovered and analyzed under NSF grants to PM (0439589, 0636506, 0829227, 1042883, 1203640), to AC (SES-86-03470, OPP-88-16912, OPP-92-19446/94-96248), and to JC-D (0337933 and 0839066). The Roosevelt Island Climate Evolution (RICE) Program ice core was funded by national contributions from New Zealand, Australia, Denmark, Germany, Italy, the People's Republic of China, Sweden, UK, and USA with logistic support provided by Antarctica New Zealand and the US Antarctic Program. This paper is a contribution to the SCAR (Scientific Committee for Antarctic Research) AntClim21 (Antarctic Climate in the 21st Century) SRP (Scientific Research Programme). All data are plotted using the Climate Change Institute's Climate Reanalyzer™.

Appendix A. Supplementary data

Supplementary data related to this article can be found at http://dx.doi.org/10.1016/j.quascirev.2016.11.017.

References

ACCE (Antarctic Climate Change and the Environment), 2009. In: Turner, J.T., Bindschadler, R., Convey, P., di Prisco, G., Fahrbach, E., Hodgson, D., Mayewski, P.A., Summerhayes, C. (Eds.), Scientific Committee for Antarctic Research, ISBN 978-0-948277-22-1.

Aitken, A.R.A., Roberts, J.L., van Ommen, T.D., et al., 2016. Repeated large-scale retreat and advance of Totten Glacier indicated by inland bed erosion. Nature 533, 385–389.

Auger, J.D., Birkel, S.D., Maasch, K.A., Mayewski, P.A., Schuenemann, K.C., 2016. An ensemble average and evaluation of third generation global climate reanalysis models. J. Geophys. Res. (in review).

Beers, T.M., Mayewski, P.A., Bertler, N.A.N., et al., 2016. 1150 Year Long Ice Core Record of the Ross Sea Polynya, Antarctica (in review).

Bertler, N.A.N., Mayewski, P.A., Sneed, S.B., et al., 2005. Solar forcing recorded by aerosol concentrations in coastal Antarctic glacier ice, McMurdo Dry Valleys.

Ann. Glaciol. 41, 52–56.
Bertler, N.A.N., Mayewski, P.A., Carter, L., 2011. Cold conditions in Antarctica during the Little Ice Age - implications for abrupt climate change mechanisms. Earth Planet. Sci. Lett. 308, 41–51.
Bracegirdle, T.J., Shuckburgh, E., Sallee, J.B., et al., 2013. Assessment of surface winds over the Atlantic, Indian, and Pacific Ocean sectors of the Southern Ocean in CMIP5 models: historical bias, forcing response, and state dependence. J. Geophys. Res. Atmos. 118, 547–562.
Bromwich, D.H., Nicolas, J.P., Monaghan, A.J., et al., 2013. Central West Antarctica among the most rapidly warming regions on Earth. Nat. Geosci. 6, 139–145.
Carleton, A.M., 1988. Sea ice-atmosphere signal of the southern oscillation in the Weddell sea, Antarctica. J. Clim. 1, 379–388.
Carleton, A.M., 1989. Antarctic sea-ice relationships with indices of the atmospheric circulation of the Southern Hemisphere. Clim. Dyn. 3, 207–220.
Carleton, A.M., 2003. Atmospheric teleconnections involving the Southern Ocean. J. Geophys. Res. - Oceans 108, 8080.
Carleton, A.M., Fitch, M., 1993. Synoptic aspects of Antarctic mesocyclones. J. Geophys. Res. 98, 12,997–13,018.
Carleton, A.M., John, G., Welsch, R., 1998. Interannual variations and regionality of Antarctic sea-ice – temperature associations. Ann. Glaciol. 27, 403–408.
Claud, C., Carleton, A.M., Duchiron, B., et al., 2009. Southern Hemisphere winter cold-air mesocyclones: climatic environments and associations with teleconnections. Clim. Dyn. 33, 383–408.
Clement, A., Bellomo, K., Murphy, L.N., et al., 2015. The Atlantic Multidecadal Oscillation without a role for ocean circulation. Science 350, 320–324.
Connolley, W.M., 1997. Variability in annual mean circulation in southern high latitudes. Clim. Dyn. 13, 745–756.
Conway, H., Hall, B.L., Denton, G.H., et al., 1999. Past and future grounding- line retreat of West Antarctic ice sheet. Science 286, 280–283.
Criscitiello, A.S., Das, S.B., Karnauskas, K.B., et al., 2014. Tropical Pacific influence on the source and transport of marine aerosols to West Antarctica. J. Clim. 27, 1343–1363.
Cullather, R.I., Bromwich, D.H., van Woert, M.L., 1996. Interannual variations in Antarctic precipitation related to El Niño-southern oscillation. J. Geophys. Res. 101, 19,109–19,118.
Ding, Q., Steig, E.J., Battisti, D.S., et al., 2011. Winter warming in West Antarctica caused by central tropical Pacific warming. Nat. Geosci. 4, 398–403.
Dixon, D.A., Mayewski, P.A., Goodwin, I., et al., 2012. An ice-core proxy for northerly air mass incursions into West Antarctica. Int. J. Climatol. 32, 1455–1465.
Enomoto, H., Ohmura, A., 1990. The influences of atmospheric half-yearly cycle on the sea ice extent in the Antarctic. J. Geophys. Res. 95, 9497–9511.
Fogt, R.L., Stammerjohn, S. (Eds.), 2015. Antarctica [in "State of the Climate in 2014"], vol. 97. Bulletin of the American Meteorological Society, pp. S149–S167.
Fogt, R.L., Bromwich, D.H., Hines, K.M., 2011. Understanding the SAM influence on the south Pacific ENSO teleconnection. Clim. Dyn. 36, 1555–1576.
Fyfe, J.C., Boer, G.J., Flato, G.M., 1999. The Arctic and Antarctic Oscillations and their projected changes under global warming. Geophys. Res. Lett. 26, 1601–1604.
Gong, D., Wang, S., 1999. Definition of Antarctic oscillation index. Geophys. Res. Lett. 26, 459–462.
Greenbaum, J.S., Blankenship, D.D., Young, D.A., et al., 2015. Ocean access to a cavity beneath Totten glacier in East Antarctica. Nat. Geosci. 8, 294–298.
Henley, B.J., Gergis, J., Karoly, D.J., et al., 2015. A Tripole index for the Interdecadal Pacific oscillation. Clim. Dyn. 45, 3077–3090.
Herron, M.M., 1982. Impurities of fluoride, chloride, nitrate and sulfate in Greenland and Antarctic precipitation. J. Geophys. Res. Lett. 87, 3052–3060.
Holland, P.R., Kwok, R., 2012. Wind-driven trends in Antarctic sea-ice drift. Nat. Geosci. 5, 872–875.
Jiang, S., Cole-Dai, J., Li, Y., et al., 2012. A detailed 2840-year record of explosive volcanism in a shallow ice core from Dome A, East Antarctica. J. Glaciol. 58, 65–75.
Jungclaus, J.H., Haak, H., Latif, M., et al., 2005. Arctic-North Atlantic interactions and multidecadal variability of the meridional overturning circulation. J. Clim. 18, 4013–4031.
Kaspari, S., Mayewski, P.A., Dixon, D., et al., 2005. Sources and transport pathways for marine aerosol species into West Antarctica. Ann. Glaciol. 41, 1–9.
Korotkikh, E.V., Mayewski, P.A., Kurbatov, A.V., Handley, M.J., Sneed, S.B., Dixon, D., Potocki, M., 2016. Natural and Anthropogenic Source Arsenic Partitionned Using an ~2060 Year Long South Pole Ice Core (in review).
Knigh, J.R., Allan, R.J., Folland, C.K., et al., 2005. A signature of persistent natural thermohaline circulation cycles in observed climate. Geophys. Res. Lett. 3, L20708.
Kreutz, K.J., Mayewski, P.A., Meeker, L.D., et al., 1997. Bipolar changes in atmospheric circulation during the Little ice Age. Science 277, 1294–1296.
Kreutz, K.J., Mayewski, P.A., Pittalwala II, et al., 2000. Sea-level pressure variability in the Amundsen Sea region inferred from a West Antarctic glaciochemical record. J. Geophys. Res. 105, 4047–4059.
Landrum, L., Holland, M.M., Schneider, D.P., et al., 2012. Antarctic sea ice climatology, variability, and Late Twentieth-Century change in CCSM4. J. Clim. 25, 4817–4838.
Large, W.G., van Loon, H., 1989. Large-scale low frequency variability of the 1979 FGGE surface buoy drifts and winds over the Southern Hemisphere. J. Phys. Oceanogr. 19, 216–232.
Legrand, M.R., Delmas, R.J., 1988. Soluble impurities in four Antarctic ice cores over the last 30,000 years. Ann. Glaciol. 10, 116–120.
Legrand, M., Mayewski, P.A., 1997. Glaciochemistry of Polar ice cores: a review. Rev. Geophys. 35, 219–243.
Maasch, K., Mayewski, P.A., Rohling, E., et al., 2005. Climate of the past 2000 years. Geogr. Ann. 87A, 7–15.
Marshall, G.J., 2003. Trends in the southern annular mode from observations and reanalyses. J. Clim. 16, 4134–4143.
Mayewski, P.A., Lyons, W.B., Zielinski, G., et al., 1995. An Ice-core-based Late Holocene History for the Transantarctic Mountains, Antarctica. Antarctic Research Series 67: Contributions to Antarctic Research IV. American Geophysical Union, pp. 33–45.
Mayewski, P.A., Rohling, E., Stager, C., et al., 2004. Holocene climate variability. Quat. Res. 62, 243–255.
Mayewski, P.A., Maasch, K., Yan, Y., et al., 2006. Solar forcing of the polar atmosphere. Ann. Glaciol. 41, 147–154.
Mayewski, P.A., Meredith, M., Summerhayes, C., et al., 2009. State of the Antarctic and Southern Ocean climate system (SASOCS). Rev. Geophys. 47, RG1003.
Mayewski, P.A., Maasch, K.A., Dixon, D., et al., 2013. West Antarctica's sensitivity to natural and human-forced climate change over the Holocene. J. Quat. Sci. 28, 40–48.
Mayewski, P.A., Bertler, N., Birkel, S., et al., 2015. Potential for southern hemisphere climate surprises. J. Quat. Sci. (Rapid Commun. 30, 391–395.
Mo, K.C., Ghil, M., 1987. Statistics and dynamics of persistent anomalies. J. Atmos. Sci. 44, 877–901.
Mo, K.C., Higgins, R.W., 1998. The Pacific-South American modes and tropical convection during the Southern Hemisphere winter. Mon. Weather Rev. 126, 1581–1596.
Monselesan, D.P., O'Kane, T.J., Risbey, J.S., et al., 2015. Internal climate memory in observations and models. Geophys. Res. Lett. 42, 1232–1242.
Nicolas, J.P., Bromwich, D.H., 2011. Climate of West Antarctica and influence of marine air mass intrusions. J. Clim. 24, 49–67.
Orsi, A.J., Cornuelle, B.D., Severinghaus, J.P., 2012. Little ice Age cold interval in West Antarctica: evidence from borehole temperature at the west Antarctic ice sheet (WAIS) Divide. Geophys. Res. Lett. 39, L09710.
Pedro, J.B., Martin, T., Steig, E.J., et al., 2016. Southern Ocean deep convection as a driver of Antarctic warming events. Geophys. Res. Lett. 43, 2192–2199.
Pittock, A.B., 1984. On the reality, stability, and usefulness of Southern Hemisphere teleconnections. Aust. Meteorol. Mag. 32, 75–82.
Plummer, C.T., Curran, M.A.J., van Ommen, T.D., et al., 2012. An independently dated 2000-year volcanic record from Law Dome, East Antarctica, including a new perspective on the dating of the c. 1450s eruption of Kuwae, Vanuatu. Clim. Past 8, 1929–1940. http://dx.doi.org/10.5194/cp-8-1929-2012.
Polvani, L.M., Waugh, D.W., Correa, G.J.P., et al., 2011. Stratospheric ozone depletion: the main driver of twentieth-century atmospheric circulation changes in the Southern Hemisphere. J. Clim. 24, 795–812.
Pritchard, H.D., Ligtenberg, S.R.M., Fricker, H.A., et al., 2012. Antarctic ice-sheet loss driven by basal melting of ice shelves. Nature 484, 502–505.
Raphael, M.N., Marshall, G.J., Turner, J., et al., 2015. The Amundsen sea low: variability, change and impact on Antarctic climate. Bull. Am. Meteorol. Soc. 97, 111–121.
Rignot, E., Mouginot, J., Morlighem, M., et al., 2014. Widespread, rapid grounding line retreat of pine Island, Thwaites, Smith, and kohler glaciers, west Antarctica, from 1992–2011. Geophys. Res. Lett. 41, 3502–3509.
Röthlisberger, R., Hutterli, M.A., Sommer, S., et al., 2000. Factors controlling nitrate in ice cores: evidence from the Dome C deep ice core. J. Geophys. Res. 105 (D16), 20,565–20,572.
Schlesinger, M.E., Ramankutty, N., 1994. An oscillation in the global climate system of period 65-70 years. Nature 367, 723–726.
Schofield, O., Ducklow, H.W., Martinson, D.G., et al., 2010. How do polar marine ecosystems respond to rapid climate change? Science 328, 1520–1523.
Schneider, D.P., Okumura, Y., Deser, C., 2012a. Observed Antarctic climate variability and tropical linkages. J. Clim. 25, 4048–4066.
Schneider, D.P., Deser, C., Okumura, Y., 2012b. An assessment and interpretation of the observed warming of West Antarctica in the austral spring. Clim. Dyn. 38, 323–347.
Shindell, D., Rind, D., Balachandran, N., et al., 1999. Solar cycle variability, ozone, and climate. Science 284, 305–308.
Shulmeister, J., Goodwin, I., Renwick, J., et al., 2004. The southern hemisphere westerlies in the Australasian sector: a synthesis. Quat. Int. 118–119, 23–53.
Sigl, M., McConnell, J.R., Layman, L., et al., 2013. A new bipolar ice core record of volcanism from WAIS Divide and NEEM and implications for climate forcing of the last 2000 years. J. Geophys. Res. 118, 1151–1169.
Sigl, M., McConnell, J.R., Toohey, M., et al., 2014. Insights from Antarctica on volcanic forcing during the common era. Nat. Clim. Change 4, 693–697.
Sigl, M., Fudge, T.J., Winstrup, M., et al., 2016. The WAIS Divide deep ice core WD2014 chronology – Part 2: annual-layer counting (0–31 Ka BP). Clim. Past 12, 769–786.
Smith, S.R., Stearns, C.R., 1993. Antarctic pressure and temperature anomalies surrounding the minimum in the Southern Oscillation Index. J. Geophys. Res. 98, 13,071–13,083.
Souney, J., Mayewski, P.A., Goodwin, I., et al., 2002. A late Holocene climate record from law Dome, east Antarctica. J. Geophys. Res. 107 (D22), 1–9.
Sneed, S.B., Mayewski, P.A., Dixon, D.A., 2011. An emerging technique: multi- ice core, multi-parameter correlations with Antarctic sea ice. Ann. Glaciol. 52, 347–354.
Spencer, P., Griffies, S.M., England, M.H., et al., 2014. Rapid subsurface warming and circulation changes of Antarctic coastal waters by poleward shifting winds.

Geophys. Res. Lett. 41, 4601–4610.
Stager, J.C., Mayewski, P.A., White, J., et al., 2012. Precipitation variability in the winter rainfall zone of South Africa during the last 1400 years linked to the austral westerlies. Clim. Past 8, 877–1125.
Steig, E.J., Hart, C.P., White, J.W.C., et al., 1998. Changes in climate, ocean and ice-sheet conditions in the Ross embayment, Antarctica at 6ka. Ann. Glaciol. 27, 305–310.
Thomas, E.R., Hosking, J.S., Tuckwell, R.R., et al., 2015. Twentieth century increase in snowfall in coastal West Antarctica. Geophys. Res. Lett. 42, 9387–9393.
Turner, J., 2004. Review, the El Niño southern oscillation and Antarctica. Int. J. Climatol. 24, 1–31.
Turner, J., Comiso, J.C., Marshall, J., 2009. Non-annular atmospheric circulation change induced by stratospheric ozone depletion and its role in the recent increase in Antarctic sea ice extent. Geophys. Res. Lett. 36, L08502.
Turner, J., Phillips, T., Hosking, S., et al., 2013. The Amundsen sea low. Int. J. Climatol. 33, 1818–1829.
Vance, T.R., van Ommen, T.D., Curran, M.A.J., et al., 2013. A millennial proxy record of ENSO and Eastern Australian rainfall from the Law Dome ice core. East Antarctica. J. Clim. 26, 710–725.
Vance, T.R., Roberts, J.L., Plummer, C.T., et al., 2015. Interdecadal Pacific variability and eastern Australian megadroughts over the last millennium. Geophys. Res. Lett. 42, 129–137.
Vance, T.R., Roberts, J.L., Moy, A.D., et al., 2016. Optimal site selection for a high-resolution ice core record in East Antarctica. Clim. Past 12, 595–610.
Van Loon, H., 1967. The half-yearly oscillations in middle and high latitudes and the coreless winter. J. Atmos. Sci. 24, 472–486.
Van Loon, H., Rogers, J.C., 1984. Interannual variations in the half-yearly cycle of pressure gradients and zonal wind at sea level on the Southern Hemisphere. Tellus 36A, 76–86.
Villalba, R., Cook, E.R., D'Arrigom, R.D., et al., 1997. Sea-level pressure variability around Antarctica since A.D. 1750 inferred from subantarctic tree-ring records. Clim. Dyn. 13, 375–390.
Whitlow, S., Mayewski, P.A., Dibb, J.E., 1992. A comparison of major chemical species input timing and accumulation at South Pole and Summit Greenland. Atmos. Environ. 26A (11), 2045–2054.
Wunsch, C., 2006. Abrupt climate change: an alternative view. Quat. Res. 64, 191–203.
Yuan, X., Martinson, D.G., 2000. Antarctic sea ice extent variability and its global connectivity. J. Clim. 13, 1697–1717.
Yuan, X., Martinson, D.G., 2001. The Antarctic Dipole and its predictability. Geophys. Res. Lett. 28, 3609–3612.
Yuan, X., Martinson, D.G., Liu, W.T., 1999. Effect of air-sea-ice interaction on winter 1996 Southern Ocean subpolar storm distribution. J. Geophys. Res. 104, 1991–2007.